

Sidereal anisotropy of GCR intensity

Latest results of two hemisphere observations by Tibet & Ice Cube

K. Munakata (Shinshu Univ., Japan)

- Latest results by Tibet & Ice Cube (Introduction)
North vs. South, Air shower vs. Muon, Energy difference....
- UG muon observations (**SK, THN**)
North-south asymmetry, Solar modulation in sub-TeV region.
- Observation & analysis method of the anisotropy
- Air shower observations with **Tibet AS array**
C-G effect in the solar time, Sidereal anisotropy, best-fit model (GA+MA model).
- Discussions

MEASUREMENT OF THE ANISOTROPY OF COSMIC RAY ARRIVAL DIRECTIONS WITH ICECUBE

ABSTRACT

We report the first observation of an anisotropy in the arrival direction of cosmic rays with energies in the multi TeV region in the Southern sky using data from the IceCube detector. Between June 2007 and March 2008, the partially-deployed IceCube detector was operated in a configuration with 1320 digital optical sensors distributed over 22 strings at depths between 1450 and 2450 meters inside the Antarctic ice. IceCube is a neutrino detector, but the data are dominated by a large background of cosmic ray muons. Therefore, the background data are suitable for high-statistics studies of cosmic rays in the Southern sky. The data include 4.3 billion muons produced by downgoing cosmic ray interactions in the atmosphere; these events were reconstructed with a median angular resolution of 3 degrees and a median energy of ~ 20 TeV. Their arrival direction distribution exhibits an anisotropy in right ascension with a first harmonic amplitude of $(6.4 \pm 0.2 \text{ stat.} \pm 0.8 \text{ syst.}) \times 10^{-4}$.

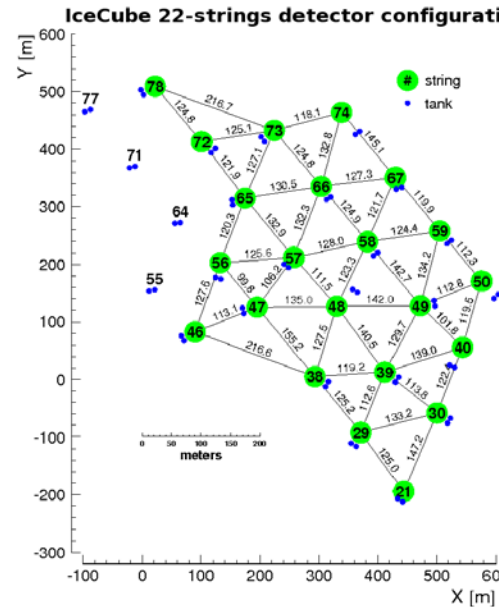
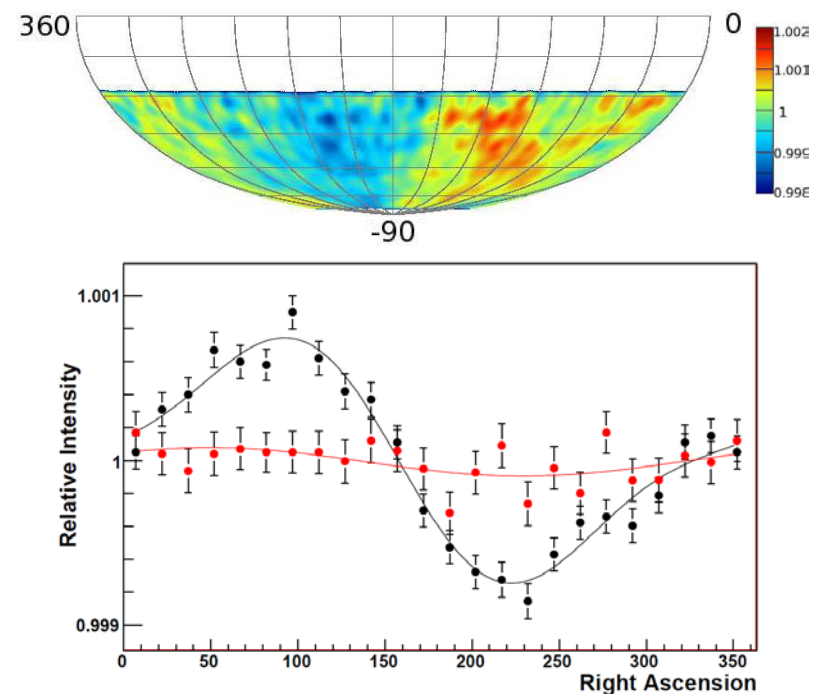


FIG. 1.— This plot shows the IceCube detector geometry in the 22 string configuration. The filled green circles are the positions of IceCube strings and the filled blue circles display the position of the IceTop tanks.

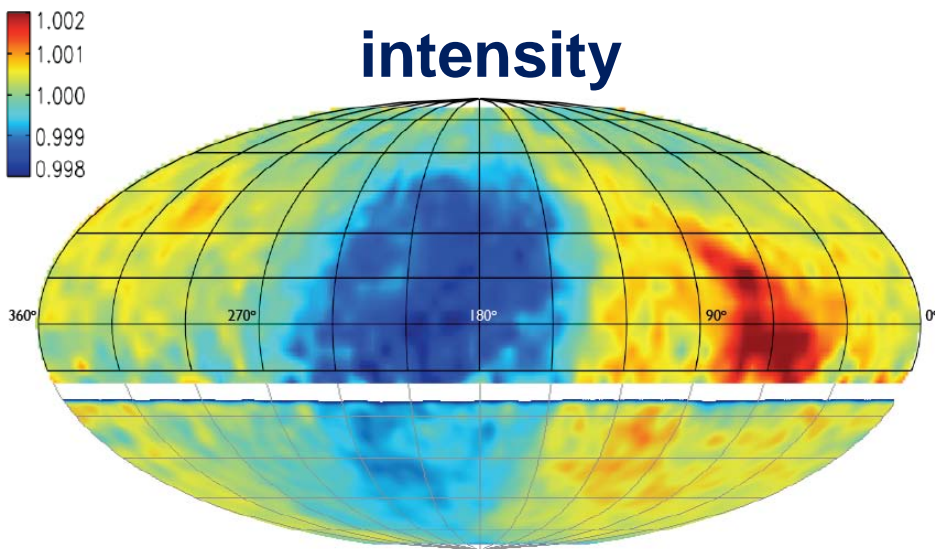


Two-hemisphere observations by Tibet & Ice Cube

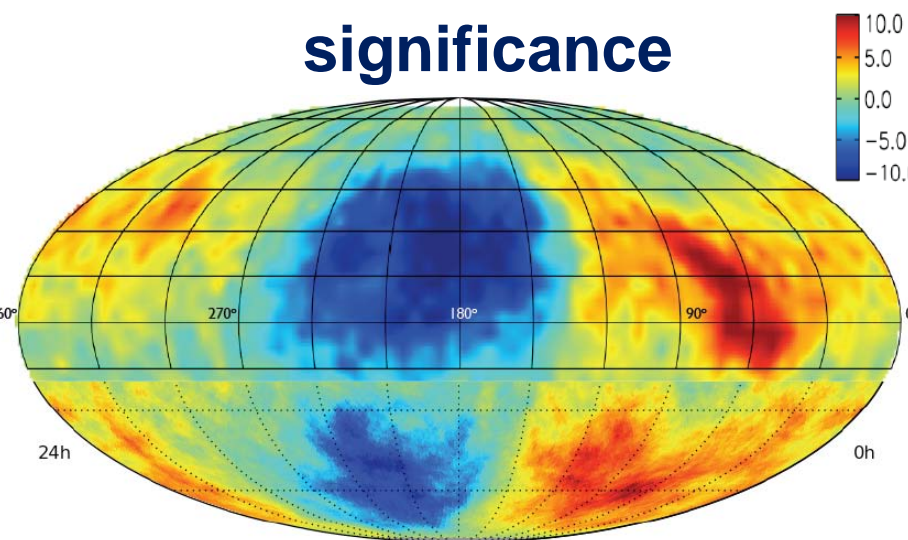
Tibet AS γ

(Amenomori et al., Science, 314, 2006)

- AS measurement ($p+\gamma$)
- $E_{\text{mode}} = 7 \text{ TeV}$ (calibrated by using Moon shadow)
- 4.5×10^{10} events in 1999.11-2008.12 (270 Hz)



intensity



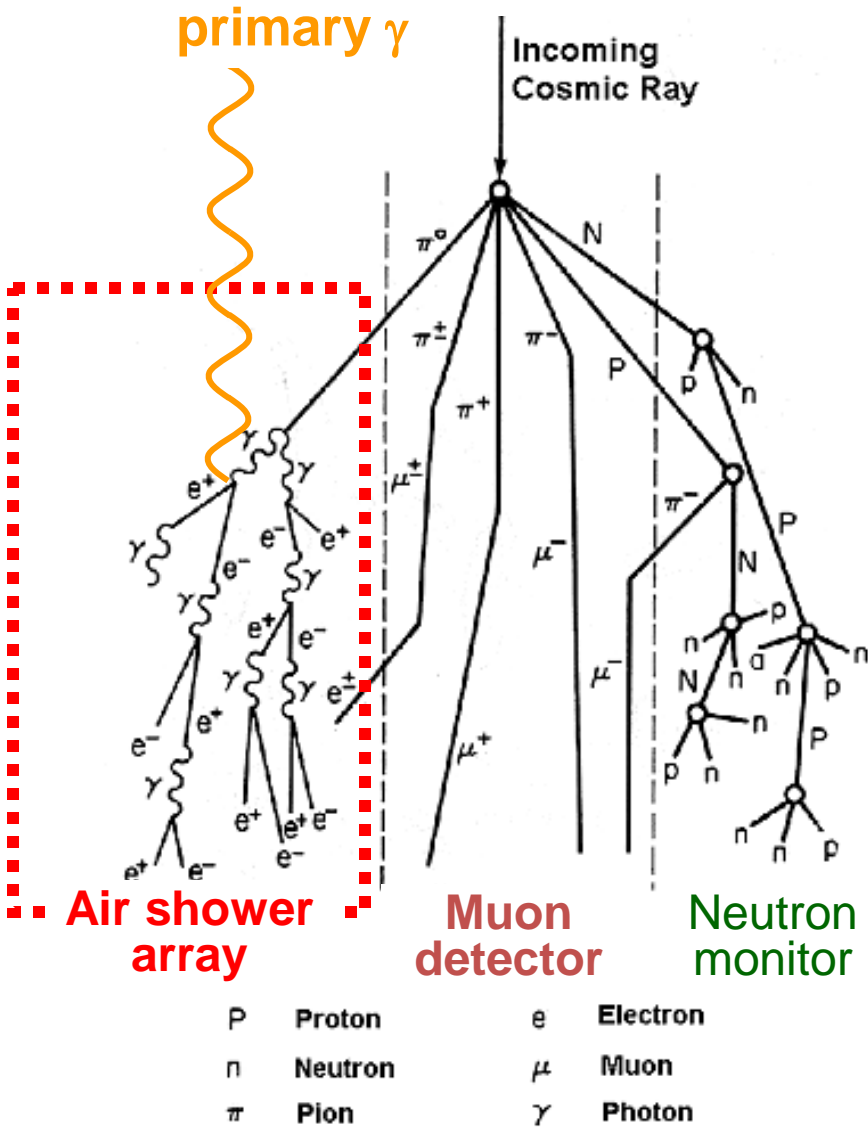
significance

Ice Cube

(Abbasi et al., arXiv:1005.2960v1, 2010)

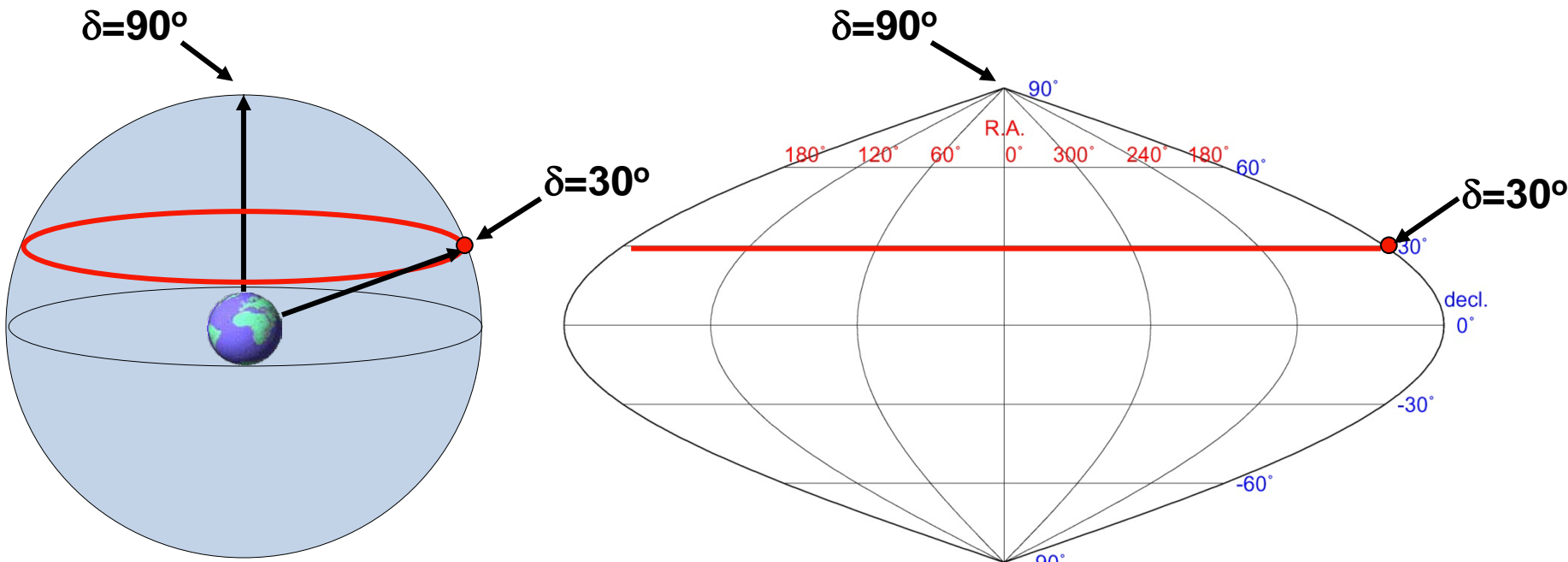
- muon measurement (p)
- $E_{\text{mode}} = 20 \text{ TeV}$
- 4.3×10^9 events in 2007.6-2008.3 (220 Hz)

Cosmic ray observation with AS array & muon detector



- **Ground-based detectors measure byproducts of the interaction of primary cosmic rays (mostly protons) with Earth's atmosphere.**
- **AS array measures electromagnetic component in the cascade shower.**
- **AS array also responds to primary γ -rays, while the muon detector responds only to primary protons & nuclei.**

Analysis method (1)



- The celestial coordinate with **declination (δ)** and **right ascension (R.A. or α)**.
- The latitude of Yangbajing in Tibet is 30°N .
The zenith direction there corresponds to $\delta=30^\circ$.

With the rotation of the Earth, the zenith direction travels the $\delta=30^\circ$ line.

- Fixed direction in the horizontal coordinate travels $\delta=\text{constant}$ line.
It returns to the same right ascension **after 1 sidereal day (360° rotation)**.

Analysis method (2)

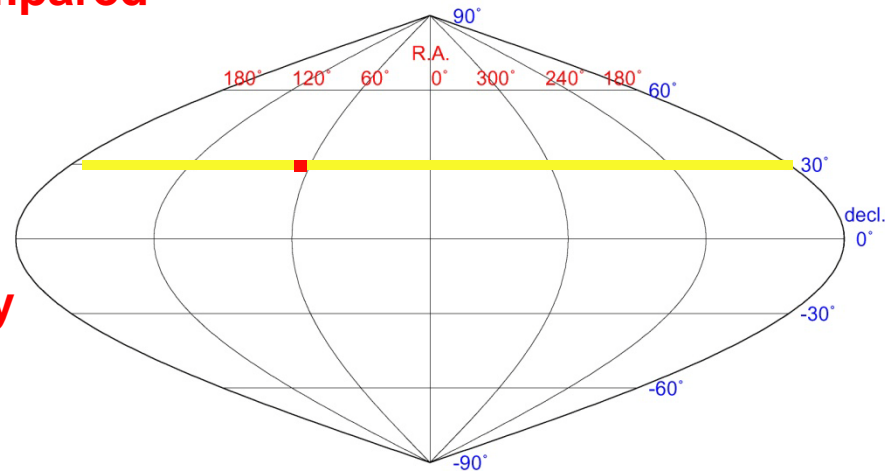
- CR flux from each celestial position is compared with average of the same declinations.

- 360° of right ascension is scanned in one sidereal day.

Time variation analysis of one sidereal day period is essential.

- Possible other time variations are:

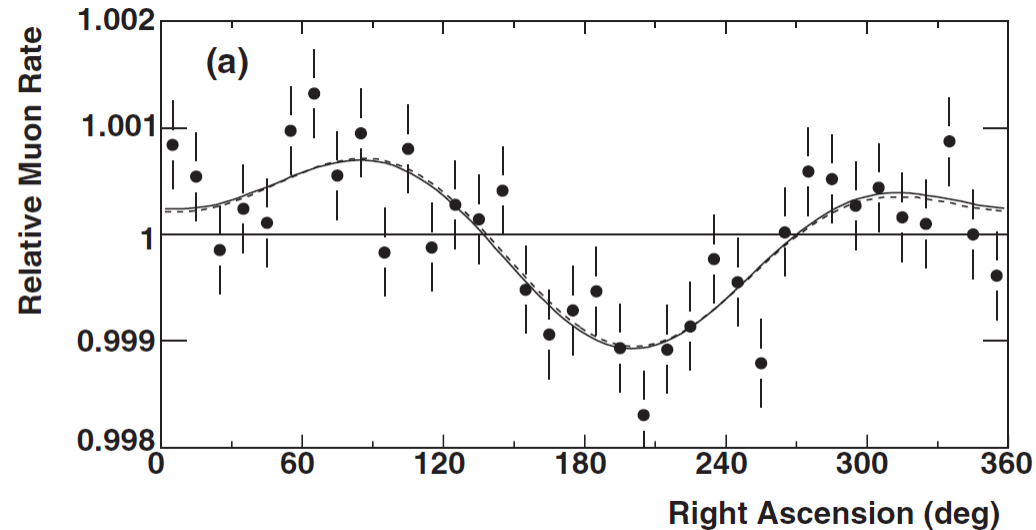
- Time variation due to the atmospheric effect.
- Time variation due to the solar modulation effect.
- An interference between one-day and one-year period variations produces fake one sidereal-day period variation.
⇒ examine anti-sidereal anisotropy



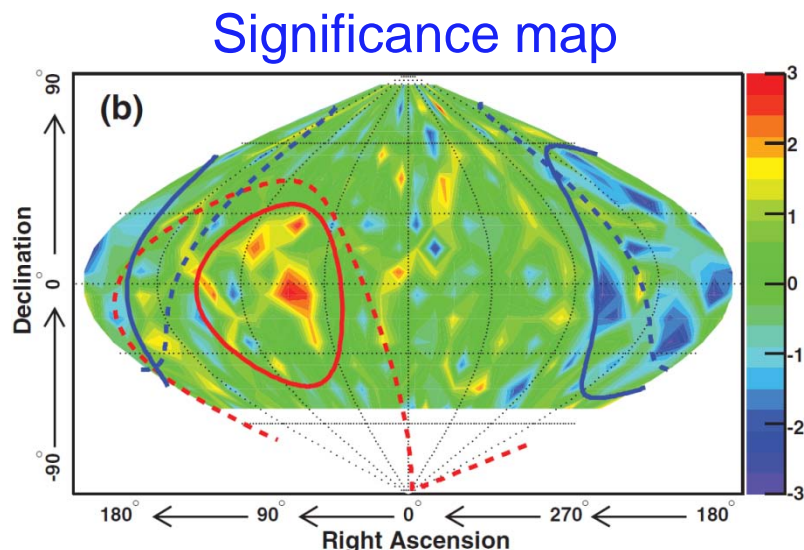
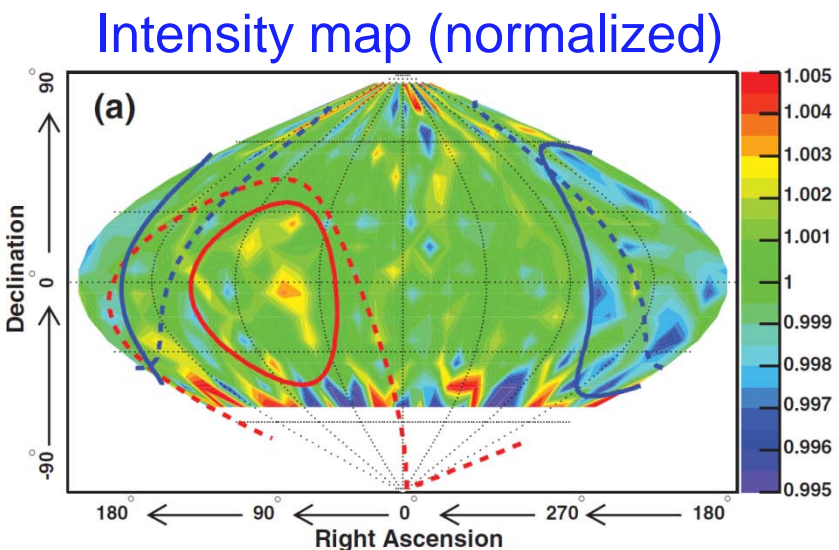
These background time variations are carefully evaluated and removed to extract primary CR anisotropy of 0.1% level.

Observation with the Super Kamiokande

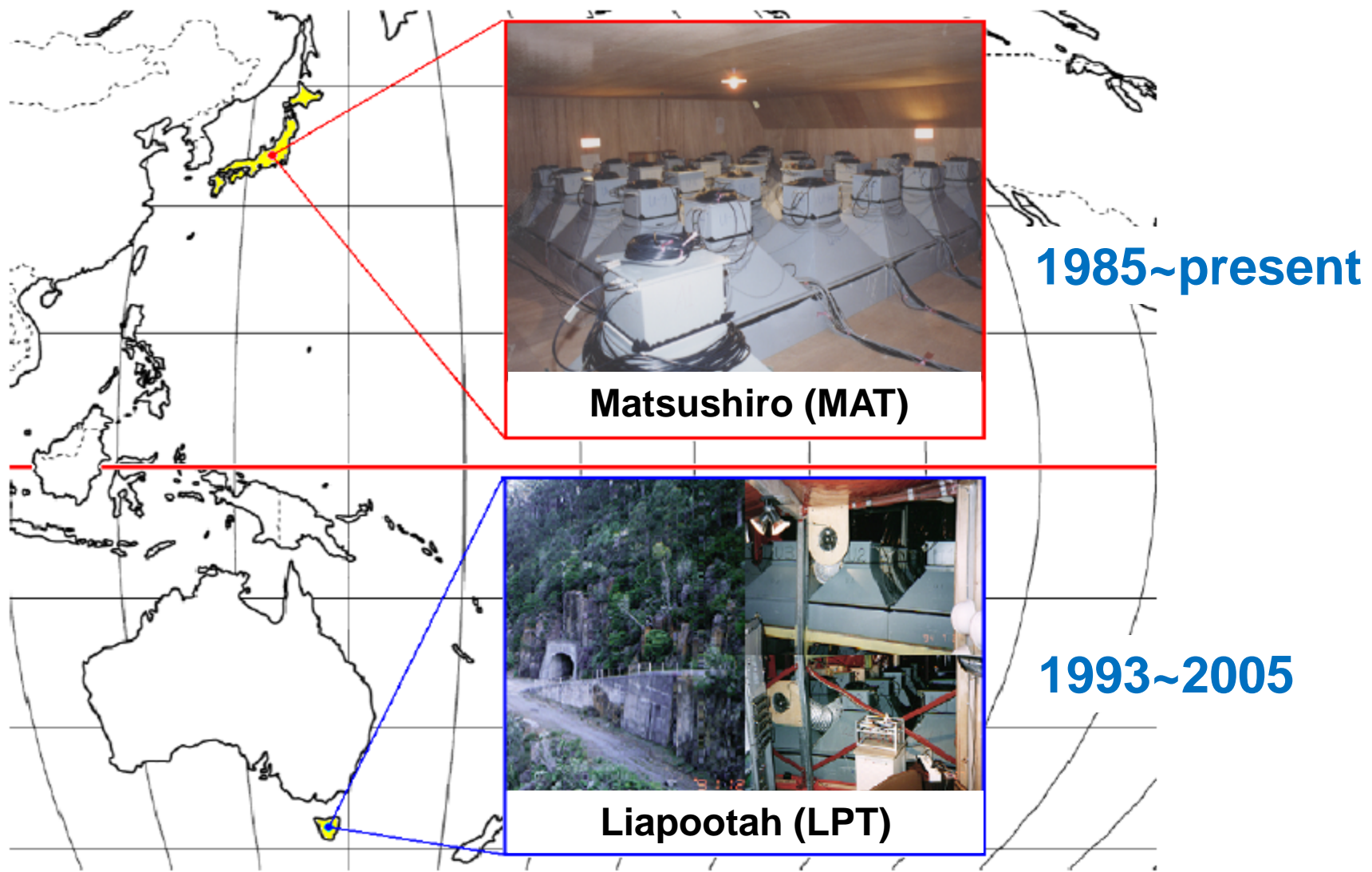
(Guillian et al., PRD., 75, 2007)



- 2.1×10^8 muons in 1996.1-2001.5 (1.8 Hz)
- $E_m = 10$ TeV
- Downward going muons (zenith angle = $0^\circ \sim 90^\circ$)



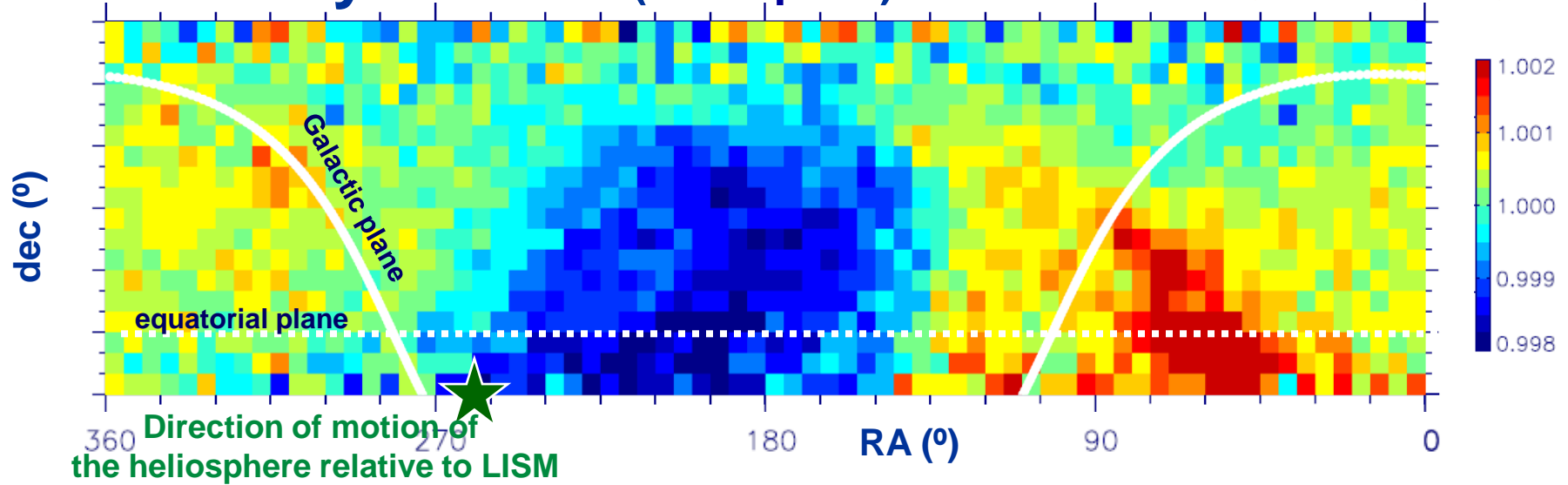
Two Hemisphere Network (THN)



Sky maps by Tibet & THN

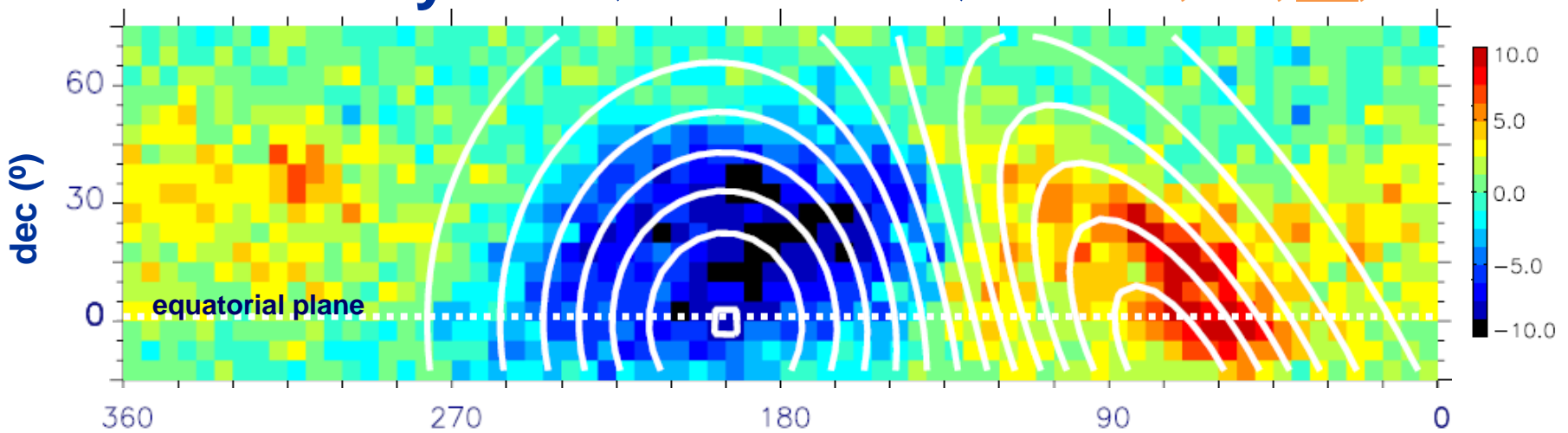
by Tibet III ($5^\circ \times 5^\circ$ pixel)

Amenomori et al., *Science*, 314, 2006



by THN (white countour)

Hall et al., *JGR*, 104, 1998



Two Hemisphere Network (THN)

Amenomori et al., arXiv0811.0422, 2008

	Matsushiro (MAT)	Liapootah (LPT)
location	36°32'N 130°01'E	42°20'S 146°28'E
V depth (m.w.e.)	220	154
count rate (Hz)	5.4	7.0
V median primary P (TV)	0.659	0.519
no. of viewing directions	17	17
Analyzed period	22 years (1985-2006)	13 years (1993-2005)

Hall et al. (JGR, 1998,1999) analyzed initial 4 years data of THN
First 2D sky-map by “Gaussian analysis”

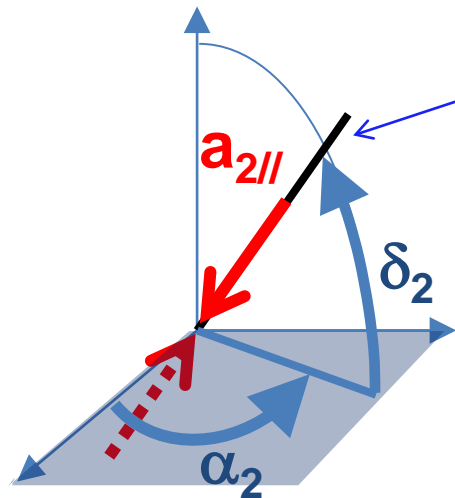
In this paper, we use the THN data updated to....

- Apply a best-fitting analysis identical to that adopted by Amenomori et al. (2007) for Tibet III data.
- Derive energy dependence of the best-fit anisotropy by comparing the best-fit parameters from the THN observation in the sub-TeV region and Tibet III experiment in the multi-TeV region.

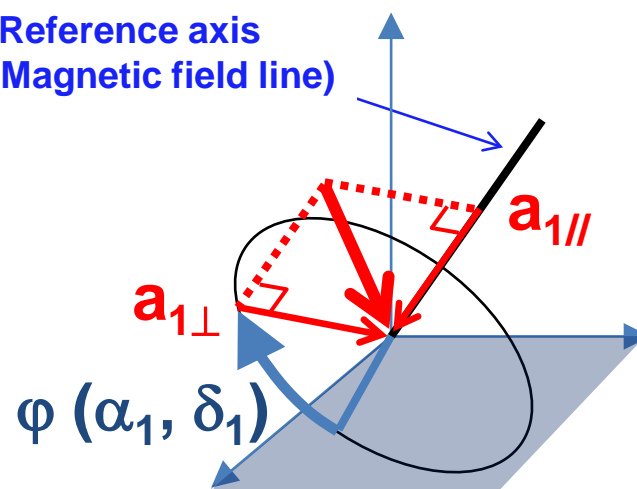
Global Anisotropy model

$$F(\theta_J, \phi_J; \theta_R, \phi_R, \theta_R^\perp, \phi_R^\perp) = \eta_1^\perp P_1^0(\cos \chi^\perp) + \eta_1^{\parallel\parallel} P_1^0(\cos \chi) + \eta_2^{\parallel\parallel} P_2^0(\cos \chi)$$

**Bi-Directional Flow
(BDF)**



**Uni-Directional Flow
(UDF)**



$$F(\theta_J, \phi_J; \theta_R, \phi_R, \theta_R^\perp, \phi_R^\perp) = \eta_1^\perp P_1^0(\cos \chi^\perp) + \eta_1^{\parallel} P_1^0(\cos \chi) + \eta_2^{\parallel} P_2^0(\cos \chi)$$

$$\begin{aligned}\cos \chi &= \cos \theta_R \cos \theta_J + \sin \theta_R \sin \theta_J \cos(\phi_J - \phi_R), \\ \cos \chi^\perp &= \cos \theta_R^\perp \cos \theta_J + \sin \theta_R^\perp \sin \theta_J \cos(\phi_J - \phi_R^\perp)\end{aligned}$$

excluding zonal terms with $P_n^0(\cos \theta_J) \dots$

$$\begin{aligned}f(\theta_J, \phi_J; \theta_R, \phi_R, \theta_R^\perp, \phi_R^\perp) &= \\ & (x_1^1 \cos \phi_J + y_1^1 \sin \phi_J) P_1^1(\cos \theta_J) \\ & + (x_2^1 \cos \phi_J + y_2^1 \sin \phi_J) P_2^1(\cos \theta_J) \\ & + (x_2^2 \cos 2\phi_J + y_2^2 \sin 2\phi_J) P_2^2(\cos \theta_J)\end{aligned}$$

$$\begin{aligned}x_1^1 &= \eta_1^\perp P_1^1(\cos \theta_R^\perp) \cos \phi_R^\perp + \eta_1^{\parallel} P_1^1(\cos \theta_R) \cos \phi_R, \\ y_1^1 &= \eta_1^\perp P_1^1(\cos \theta_R^\perp) \sin \phi_R^\perp + \eta_1^{\parallel} P_1^1(\cos \theta_R) \sin \phi_R, \\ x_2^1 &= \eta_2^{\parallel} P_2^1(\cos \theta_R) \cos \phi_R, \\ y_2^1 &= \eta_2^{\parallel} P_2^1(\cos \theta_R) \sin \phi_R, \\ x_2^2 &= \eta_2^{\parallel} P_2^2(\cos \theta_R) \cos 2\phi_R, \\ y_2^2 &= \eta_2^{\parallel} P_2^2(\cos \theta_R) \sin 2\phi_R,\end{aligned}$$

We derive the space harmonic vectors x_n^m 's
from the observed sidereal daily variations $d_{i,j}(t)$
by the j th directional channel of the i th detector

Sidereal daily variations

$$d_{i,j}(t) = \sum_{m=1}^2 (a_{m,i,j} \cos m\omega t_i + b_{m,i,j} \sin m\omega t_i),$$

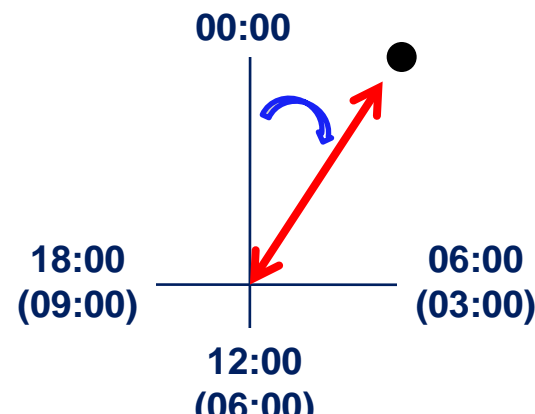
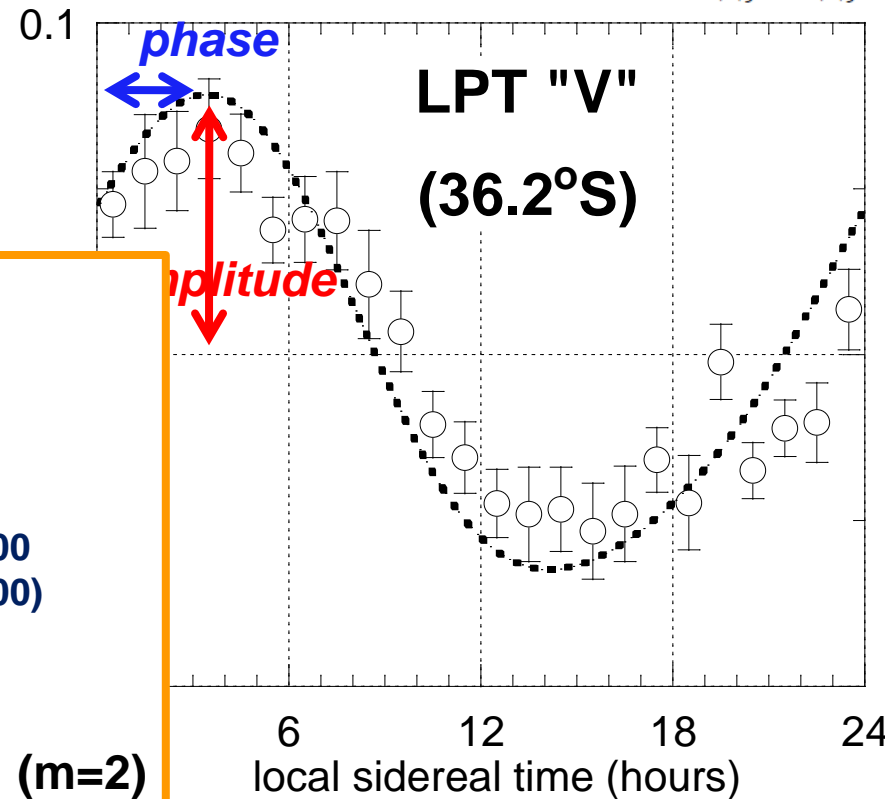
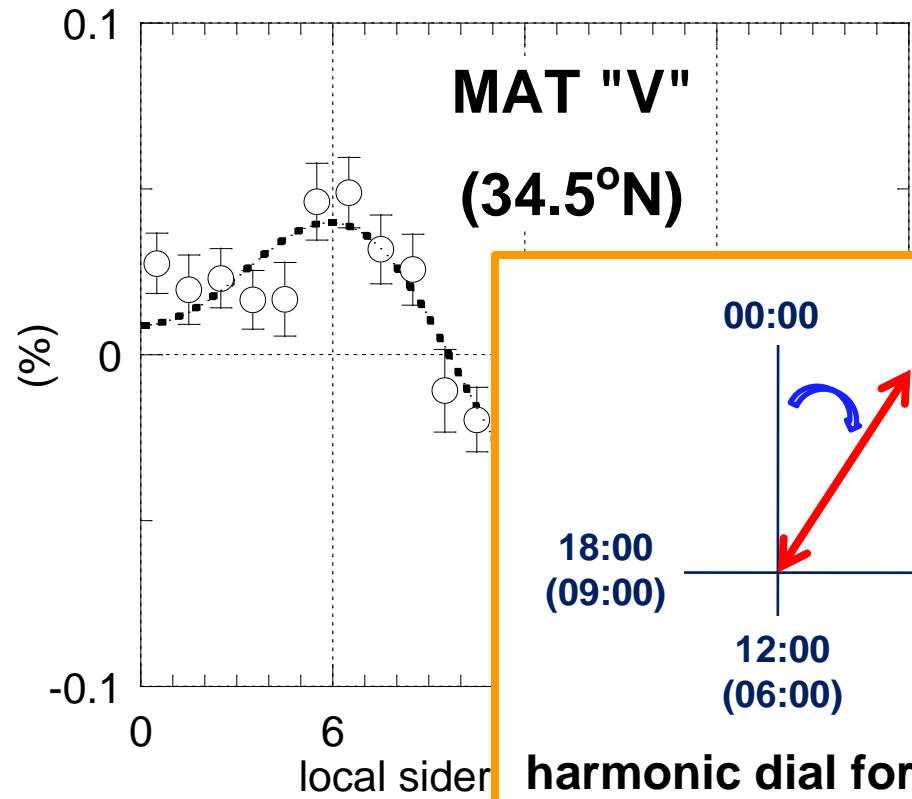
$a_{m,i,j}, b_{m,i,j}$: 136 independent data

$i = 1$ (MAT), 2 (LPT); $j = 1 \sim 17$ (V, N, S ...); $m = 1, 2$

$$\begin{aligned} a_{1i,j} &= c_{1i,j}^1 x_1^1 + s_{1i,j}^1 y_1^1 + c_{2i,j}^1 x_2^1 + s_{2i,j}^1 y_2^1, \\ b_{1i,j} &= -s_{1i,j}^1 x_1^1 + c_{1i,j}^1 y_1^1 - s_{2i,j}^1 x_2^1 + c_{2i,j}^1 y_2^1, \end{aligned}$$

$$\begin{aligned} b_{2i,j} &= -s_{2i,j}^2 x_2^2 + c_{2i,j}^2 y_2^2, \\ a_{2i,j} &= c_{2i,j}^2 x_2^2 + s_{2i,j}^2 y_2^2, \end{aligned}$$

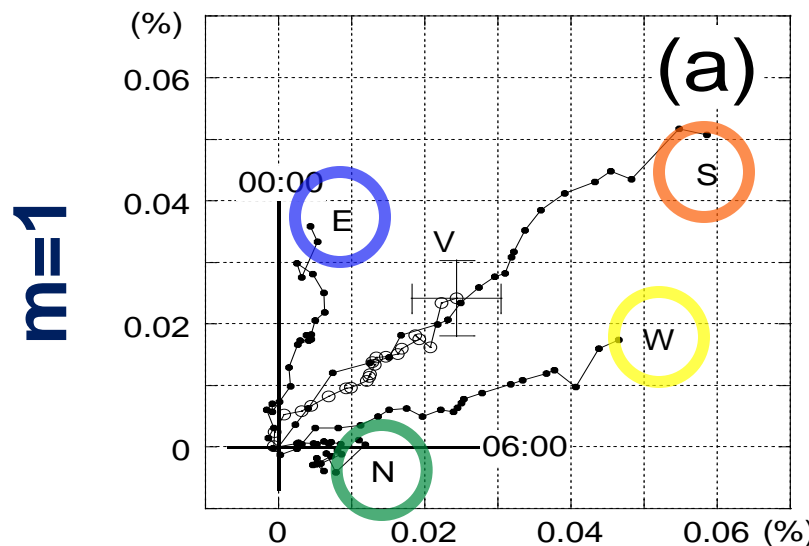
coupling coefficients: $c_{n,i,j}^m, s_{n,i,j}^m$



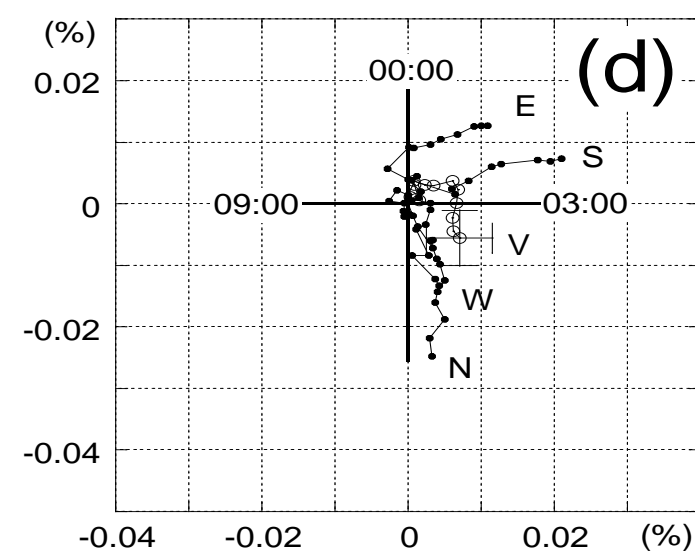
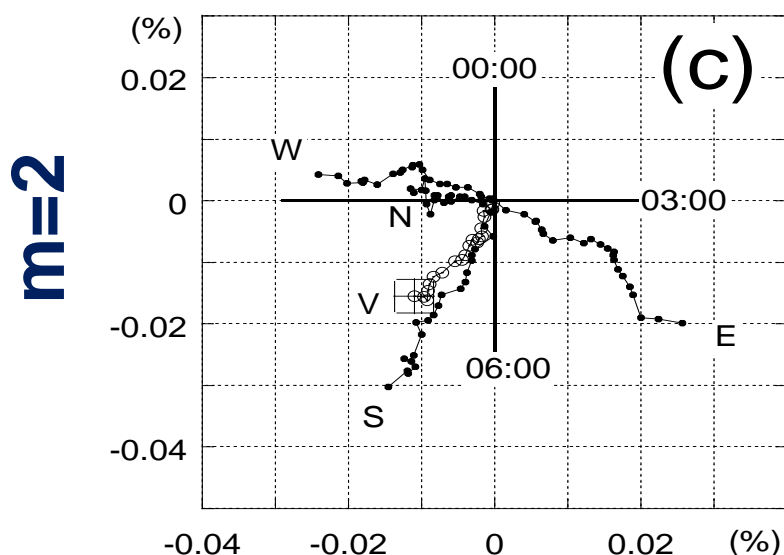
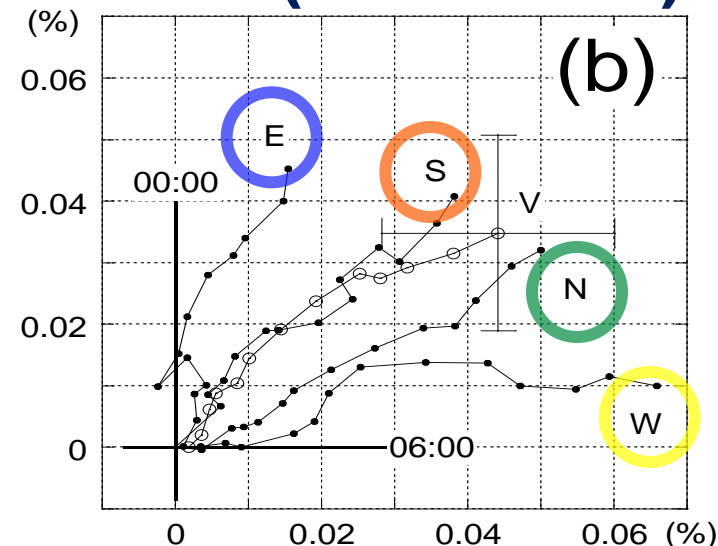
harmonic dial for $m=1$ ($m=2$)

Summation dials

MAT (1985-2006)

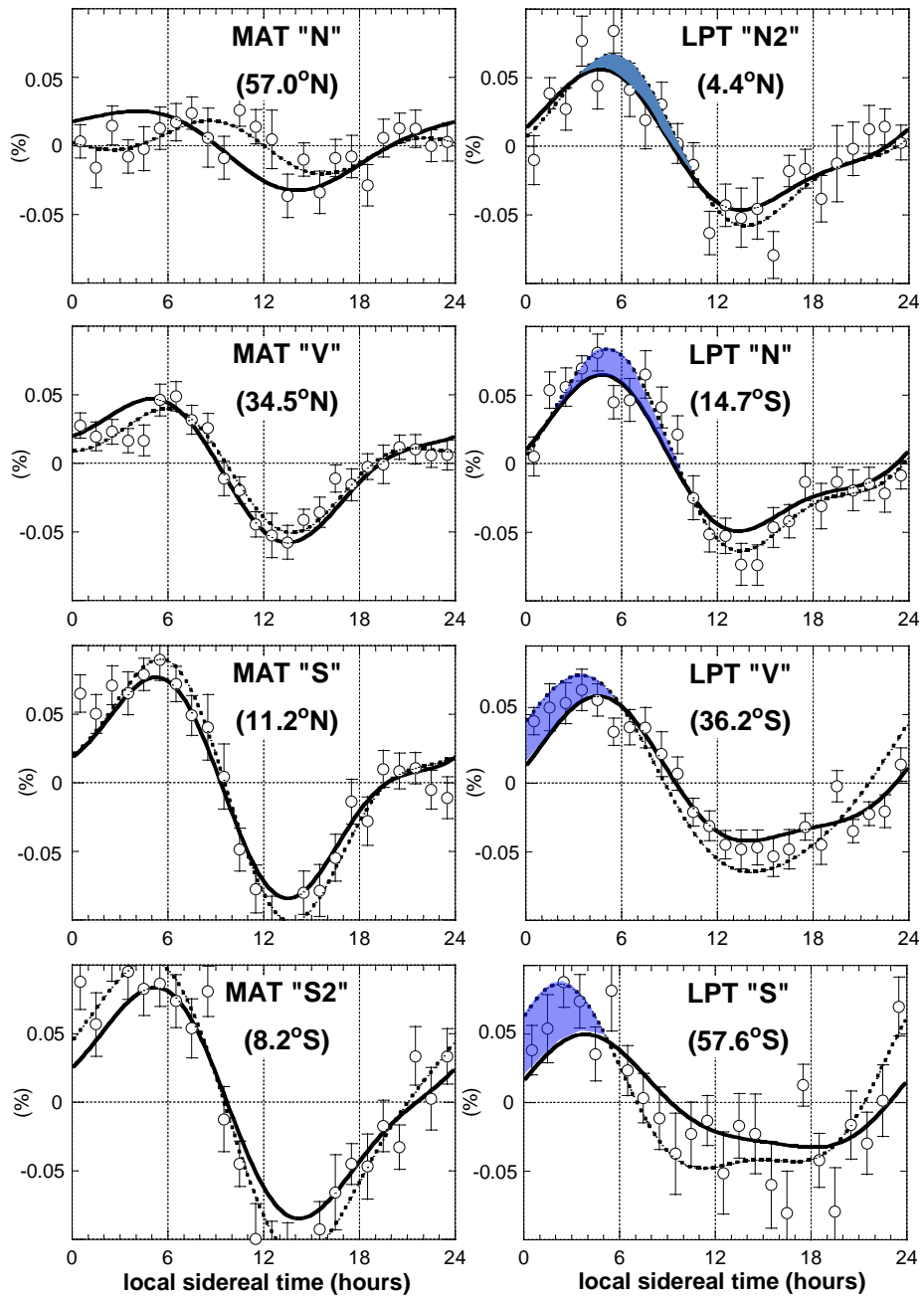


LPT (1993-2005)

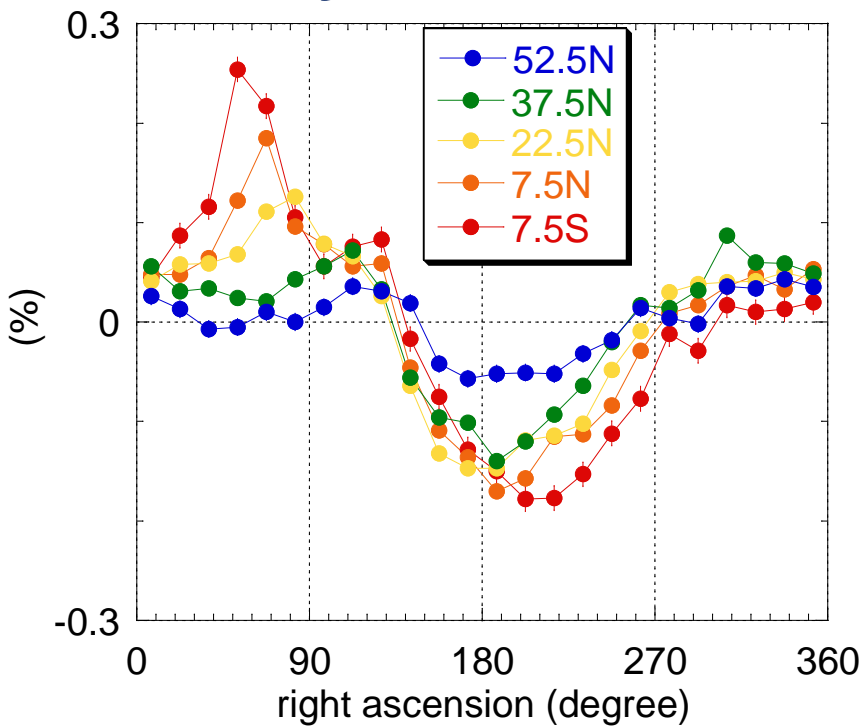


Sidereal daily variations by THN

N
↓
S



RA distribution by Tibet III

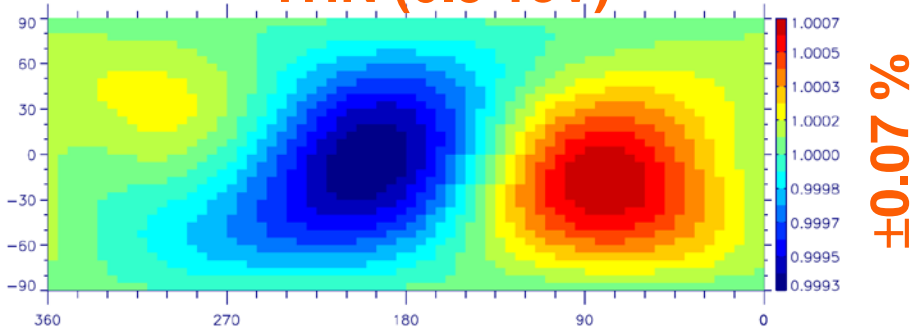


Best-fitting to THN & Tibet

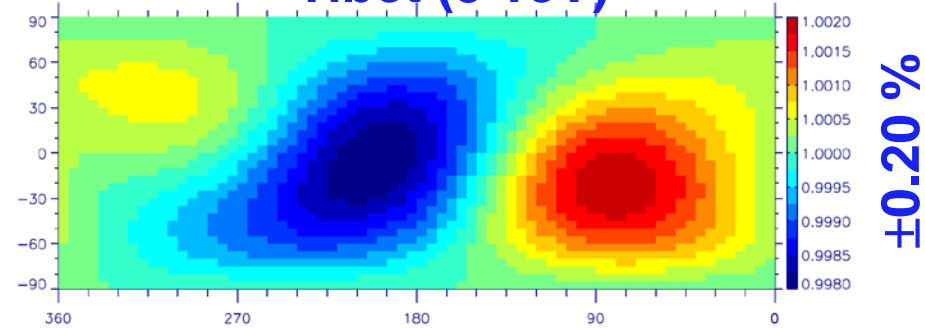
(Amenomori et al., arXiv0811.0422, 2008)

Model anisotropy

THN (0.5 TeV)



Tibet (5 TeV)



$\pm 0.07\%$

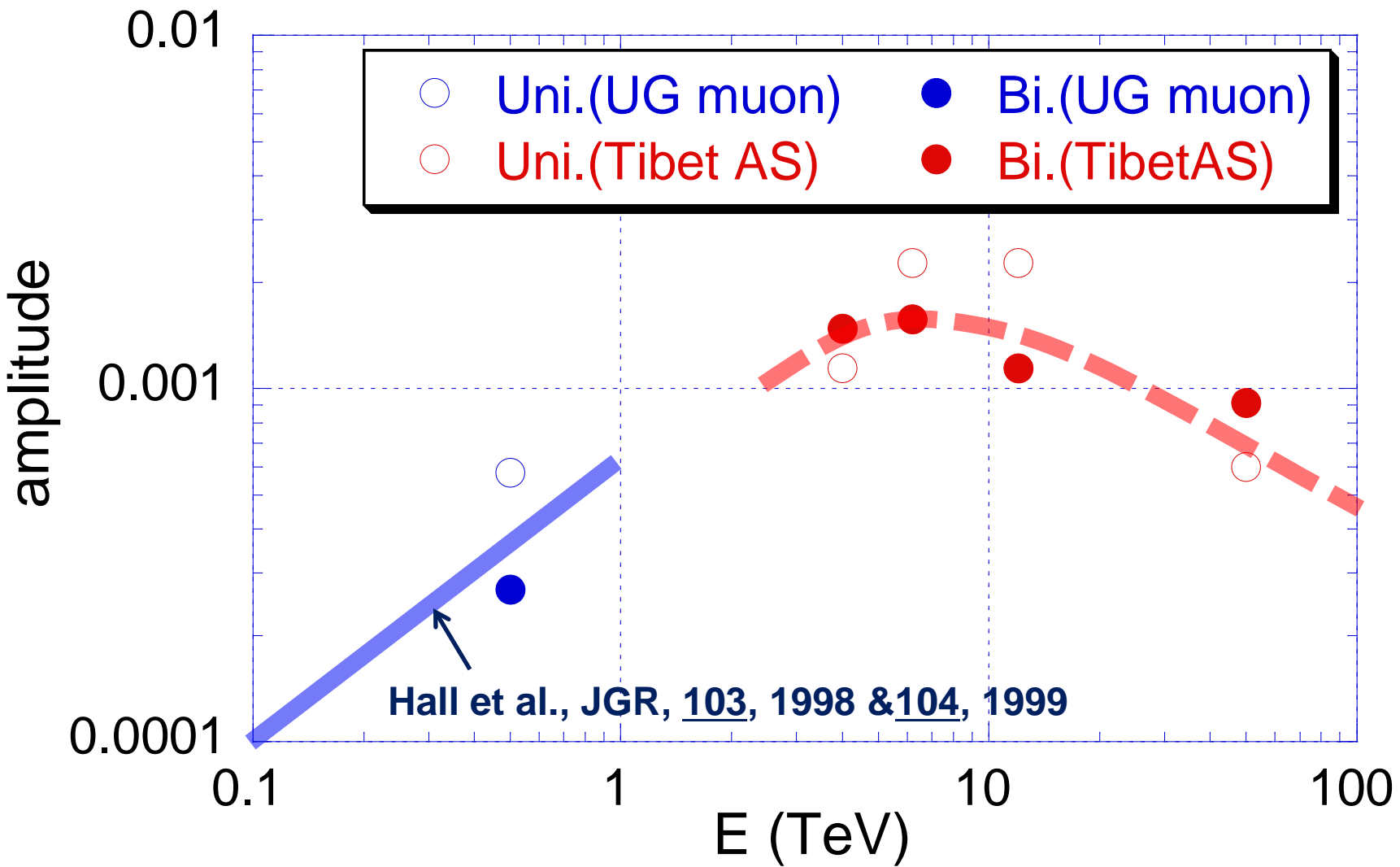
$\pm 0.20\%$

- Best-fit models of GA are very similar to each other, except 1/3 amp. by THN.
- This implies that the modeling with Tibet data in a single hemisphere is not seriously biased.

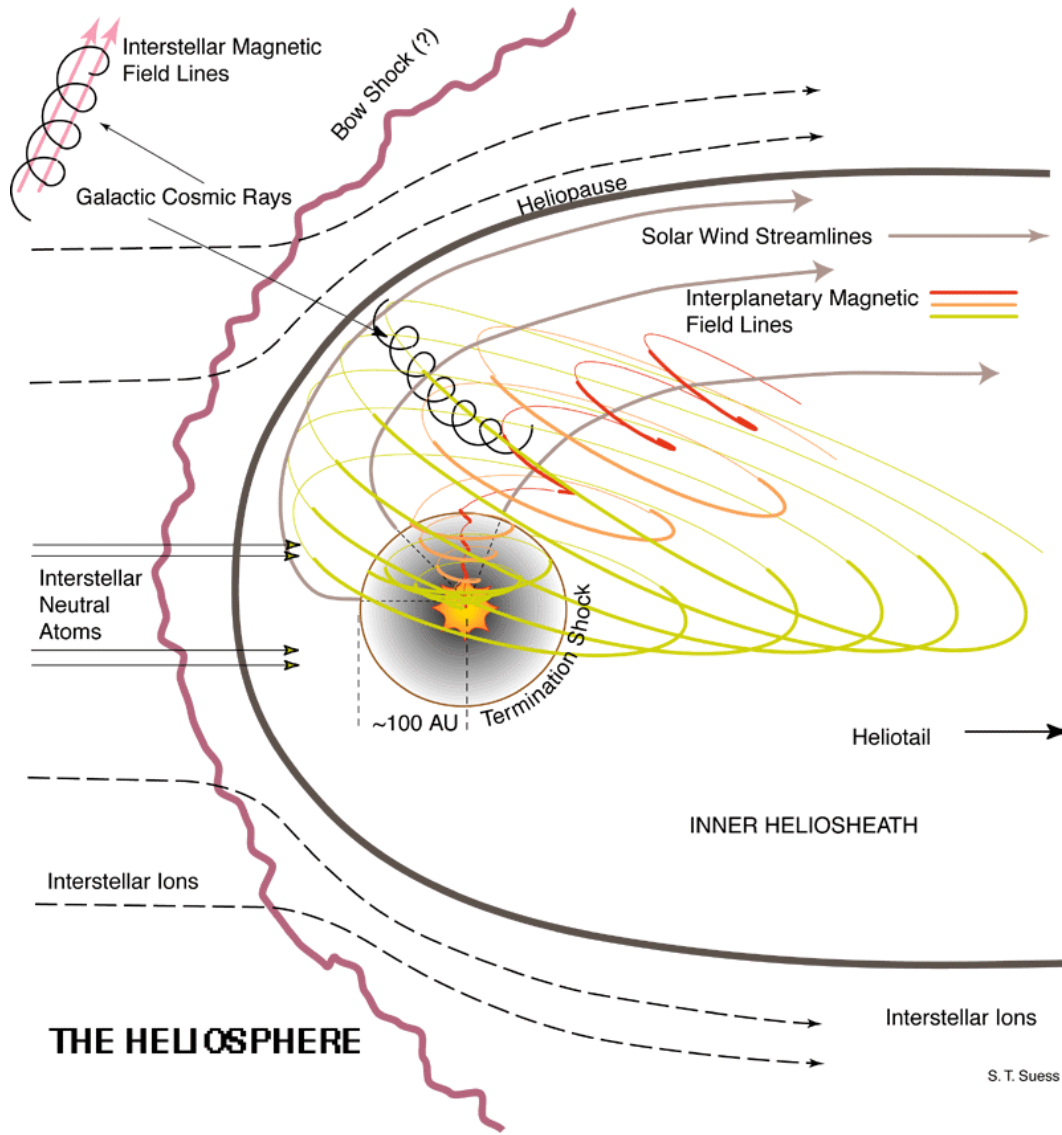
Best-fit parameters

$a_{2//}$ (%)	$\alpha_{2//}$ ($^\circ$)	$\delta_{2//}$ ($^\circ$)	$\chi^2/d.o.f. = 1.72$ $(\chi^2/d.o.f. = 2.44)$
0.020 ± 0.001 (0.095 ± 0.001)	96.4 ± 2.5 (97.4 ± 2.5)	-17.1 ± 2.5 (-22.5 ± 2.5)	
$a_{1//}$ (%)	$a_{1\perp}$ (%)	$\alpha_{1\perp}$ ($^\circ$)	$\delta_{1\perp}$ ($^\circ$)
0.016 ± 0.001 (0.096 ± 0.001)	0.020 ± 0.001 (0.108 ± 0.001)	182.5 ± 2.5 (177.5 ± 2.5)	12.5 ± 2.5 (22.5 ± 2.5)

Energy dependence of amplitude in space

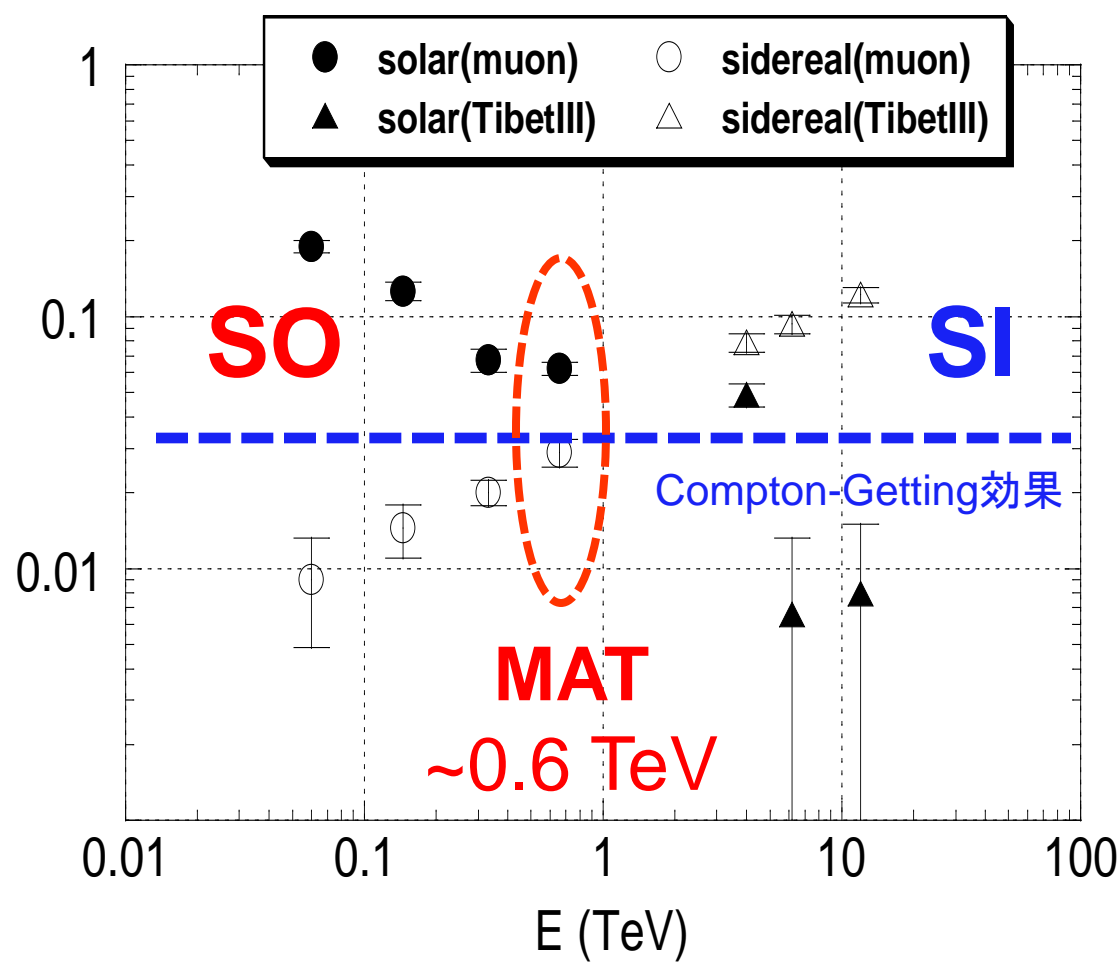
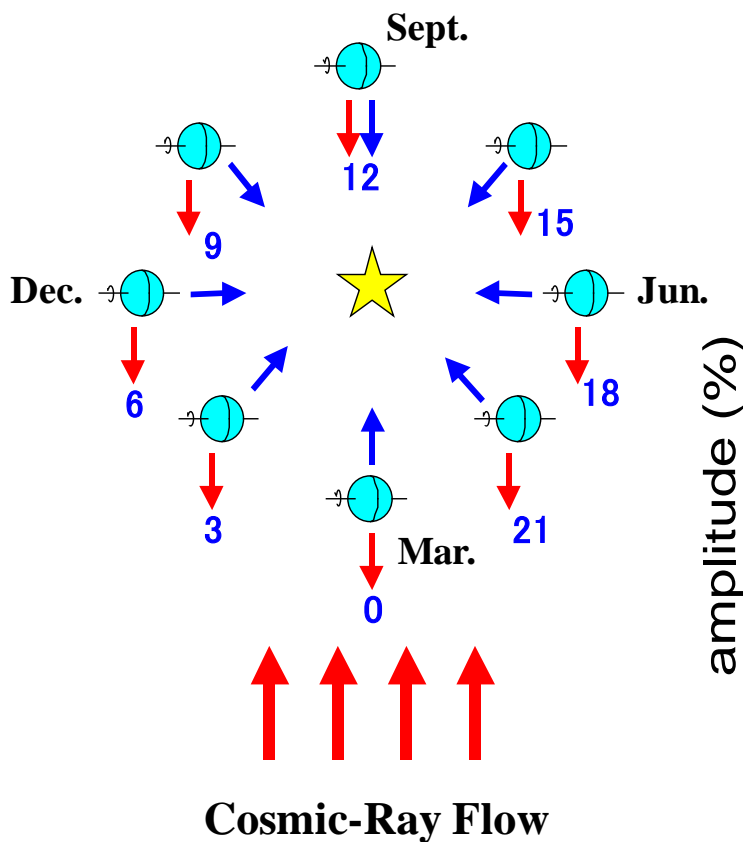


The Heliosphere



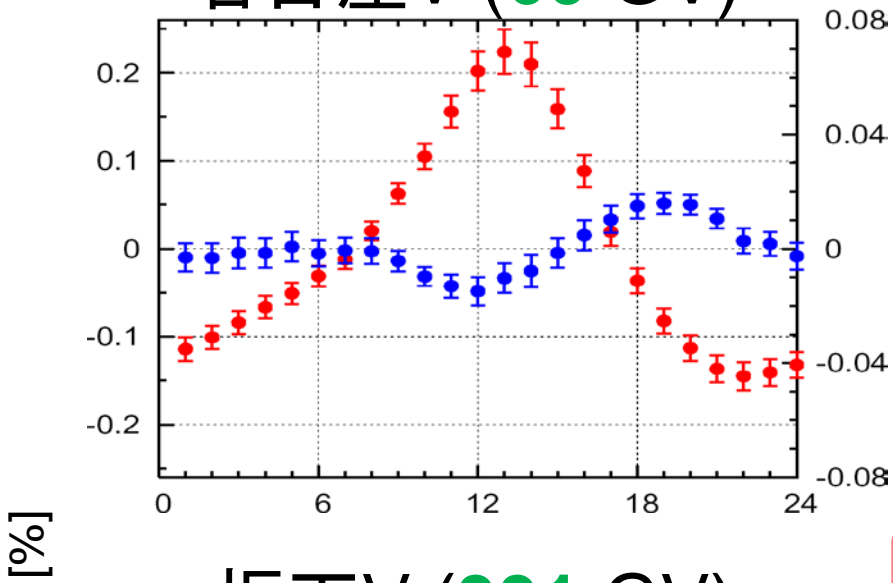
Solar modulation of solar and sidereal diurnal anisotropy

(SO: 365 c/y) (SI: 366 c/y)

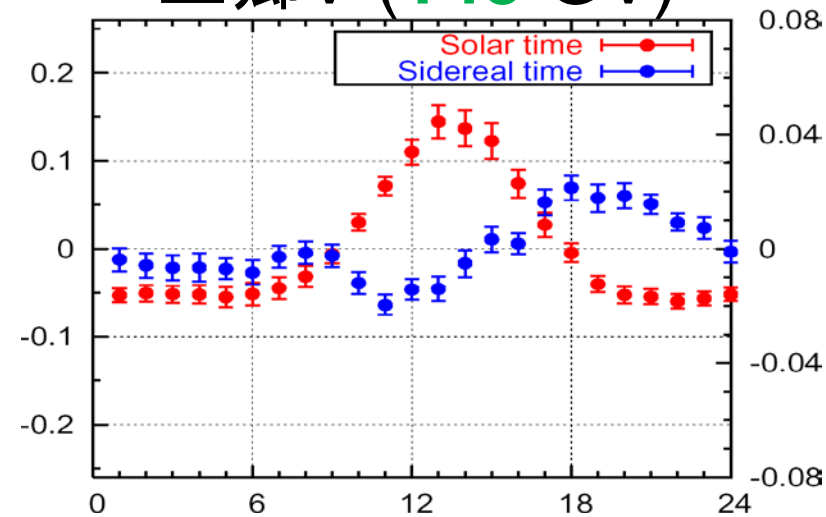


同時刻集計 in 太陽時(SO)・恒星時(SI)

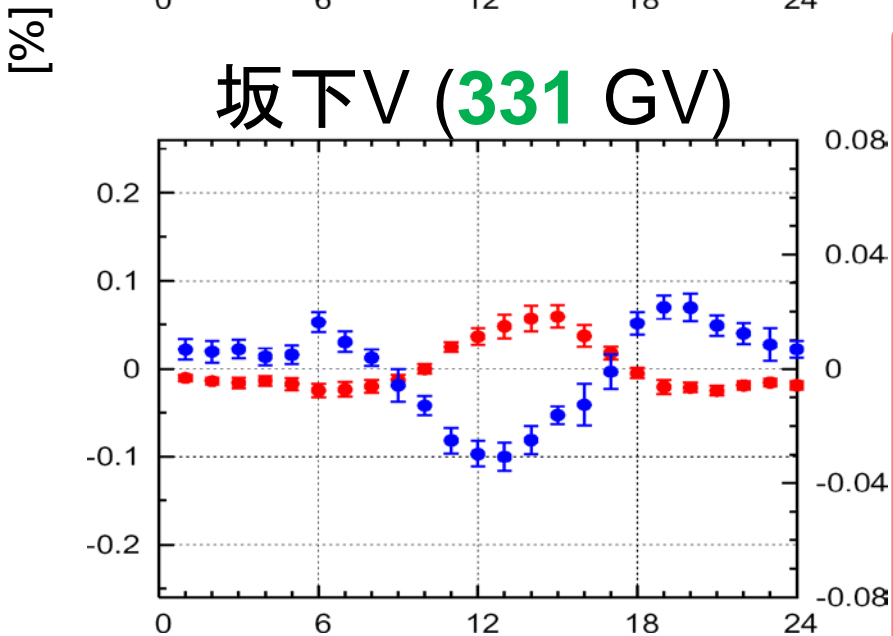
名古屋V (60 GV)



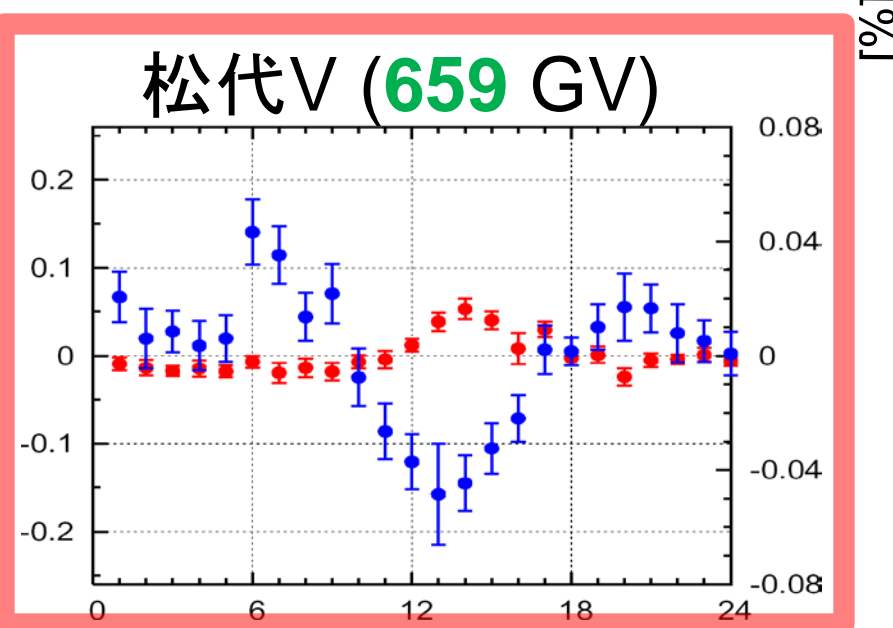
三郷V (145 GV)



坂下V (331 GV)



松代V (659 GV)



W. I. Axford

(Planetary and Space Sci., 13, 1965)

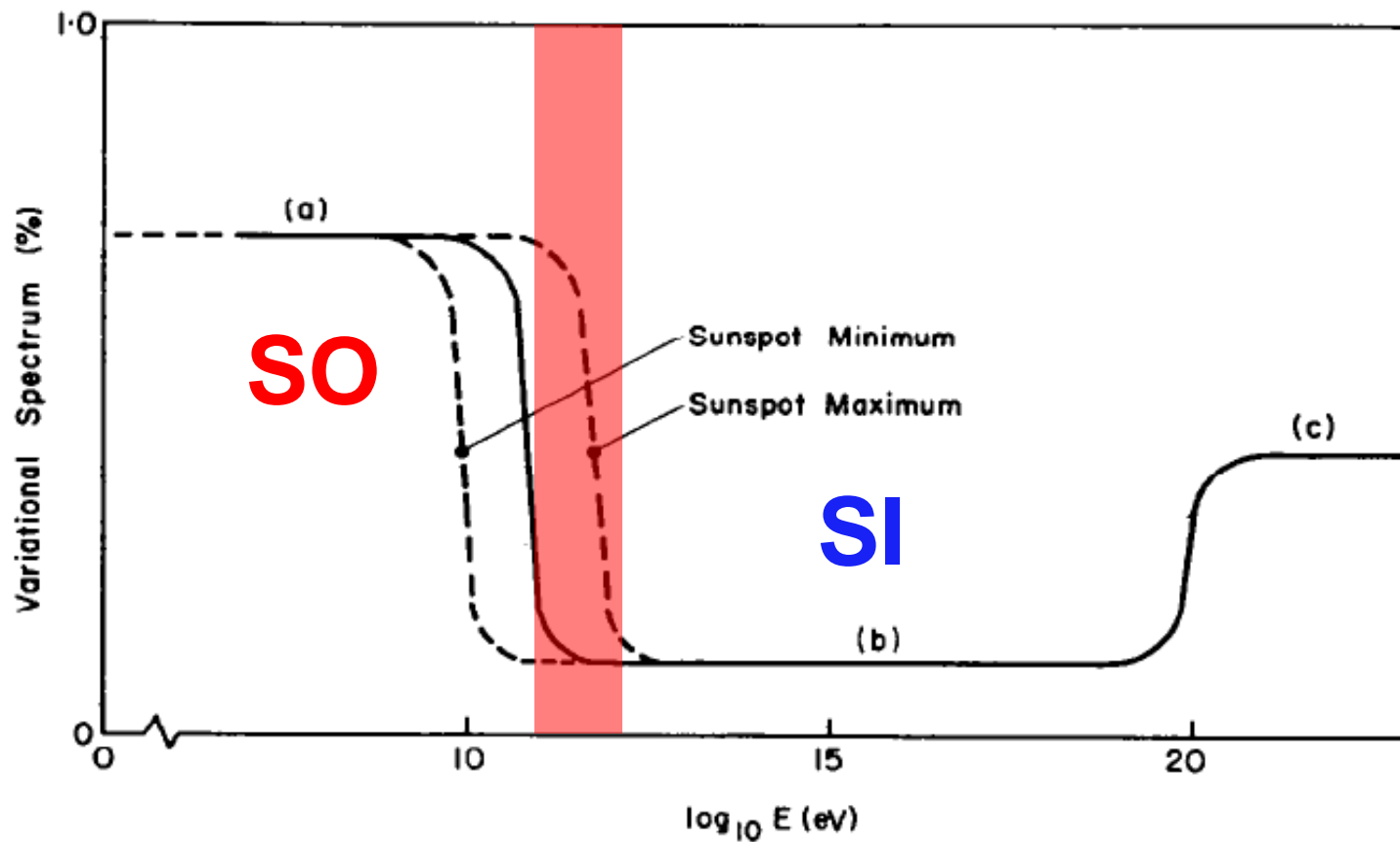


FIG. 6. SUGGESTED VARIATIONAL SPECTRUM OF THE DIURNAL MODULATION OF THE COSMIC RAY INTENSITY AT THE EARTH.

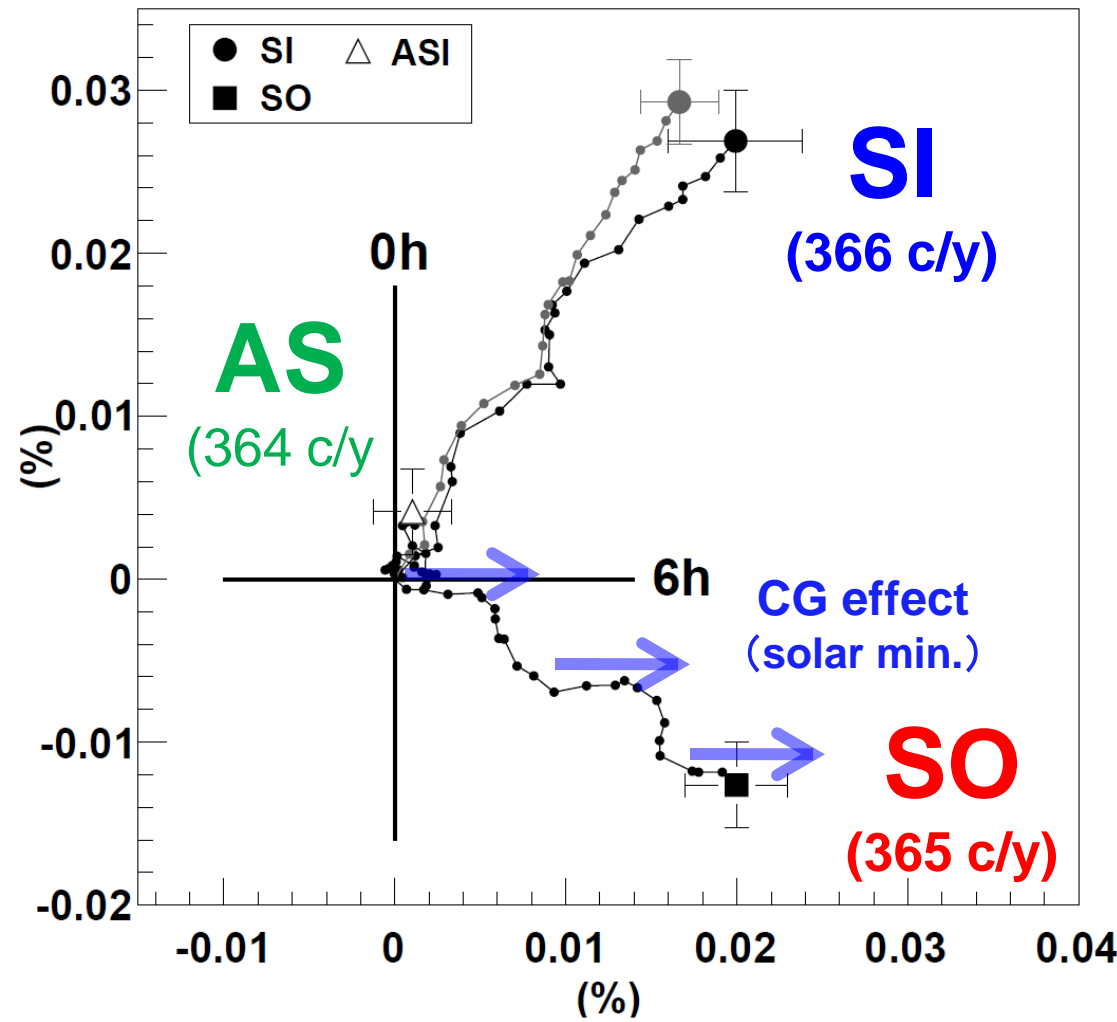
(a) REPRESENTS THE SOLAR DIURNAL VARIATION DUE TO CO-ROTATION OF THE COSMIC RAY GAS WITH THE SUN.

(b) REPRESENTS THE SIDEREAL DIURNAL VARIATION ASSOCIATED WITH STREAMING OF COSMIC RAYS WITHIN THE GALAXY, AND (c) THE SIDEREAL VARIATION DUE TO EXTRAGALACTIC EFFECTS. THE TRANSITION FROM (a) TO (b) VARIES THROUGH THE SUNSPOT CYCLE MORE OR LESS AS INDICATED.

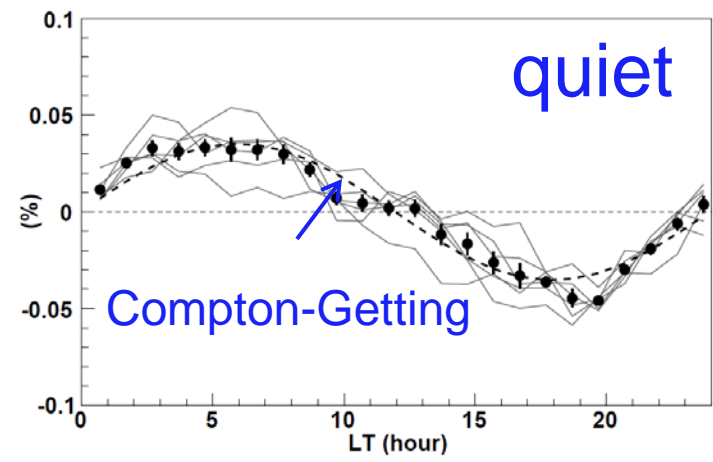
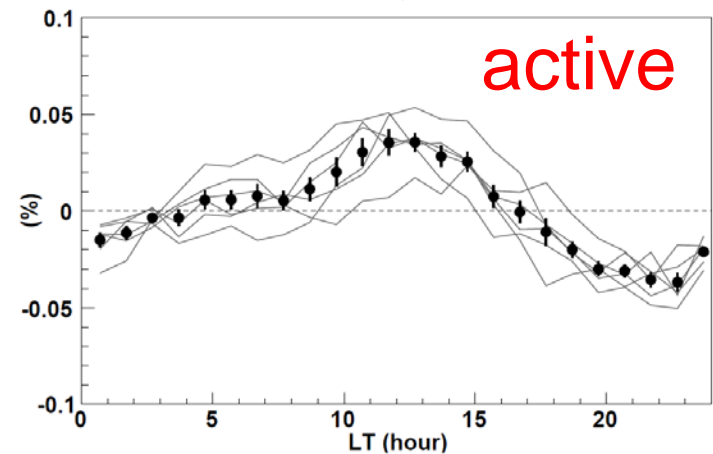
Solar cycle dependence of 0.6 TeV GCR anisotropy

(by Matsushiro UG- μ detector in 1985-2008)

Munakata et al., ApJ, 712, 2010



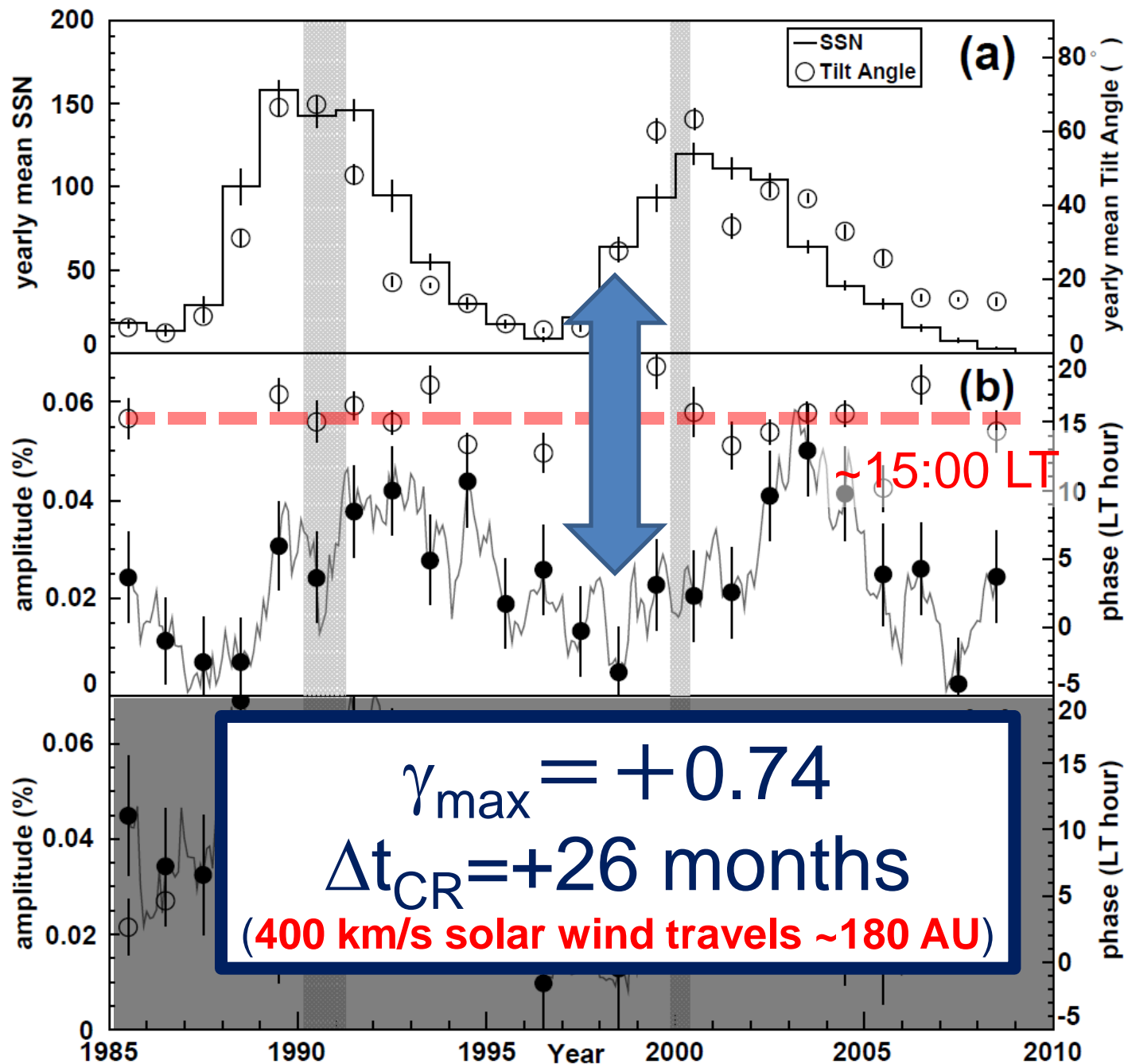
Solar daily variation



Solar activity

SO

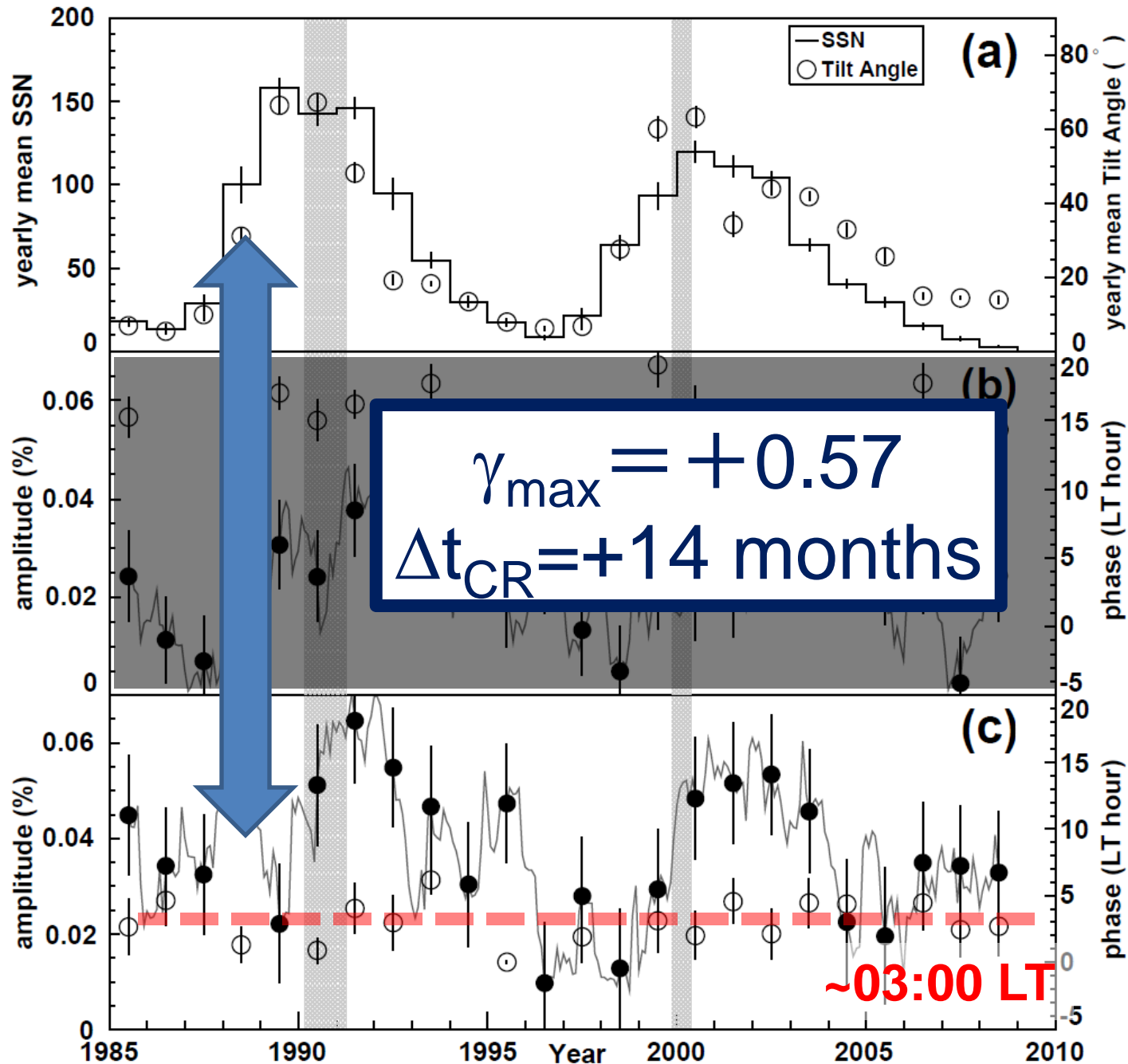
SI



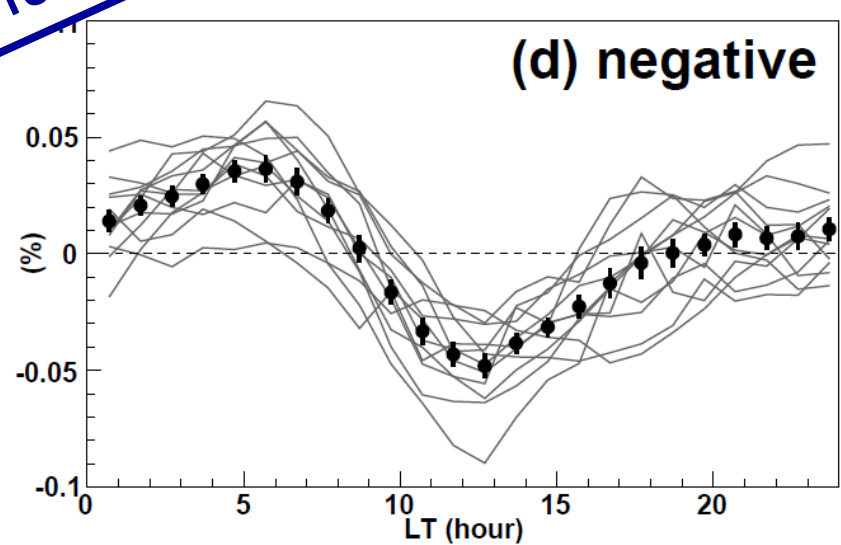
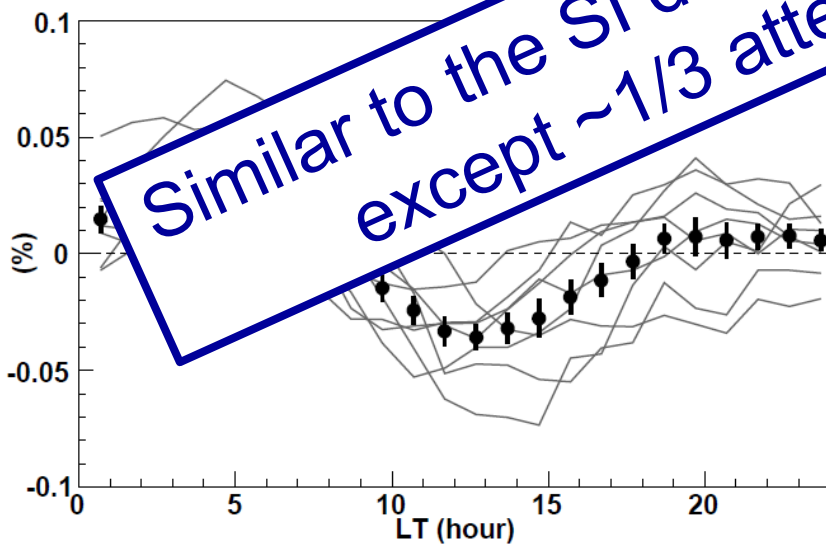
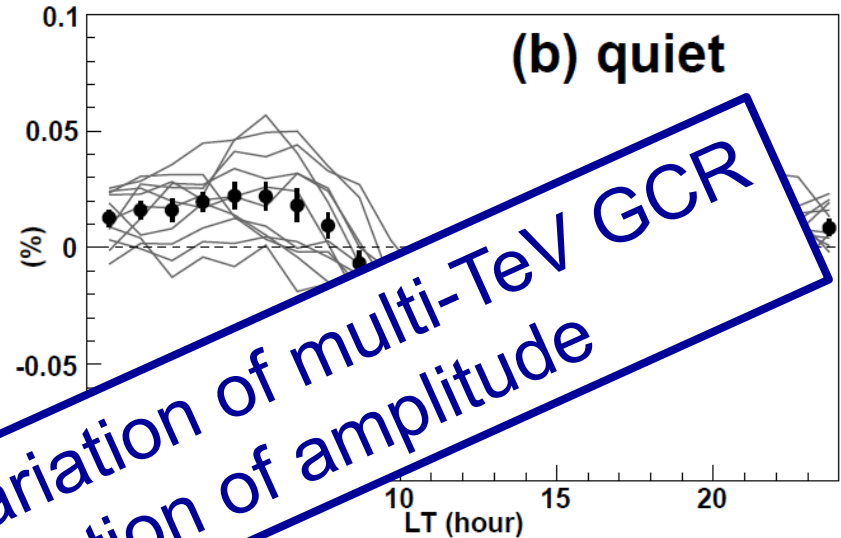
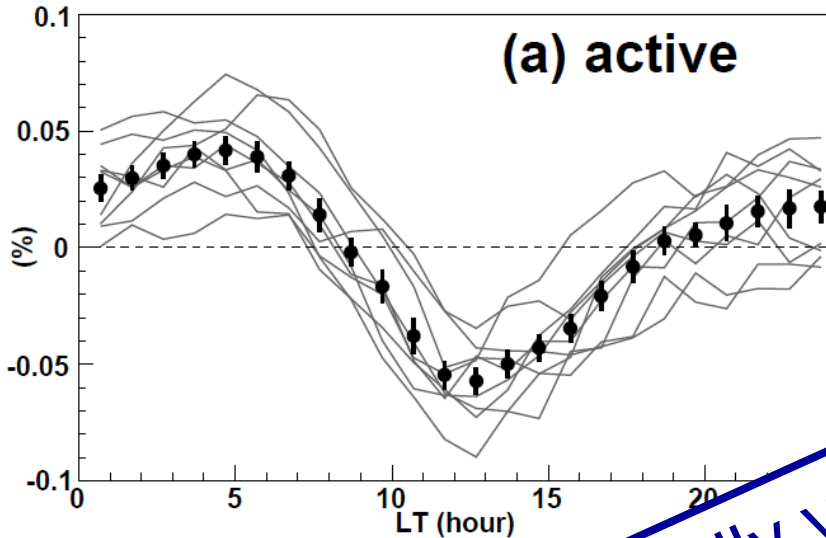
Solar activity

SO

SI

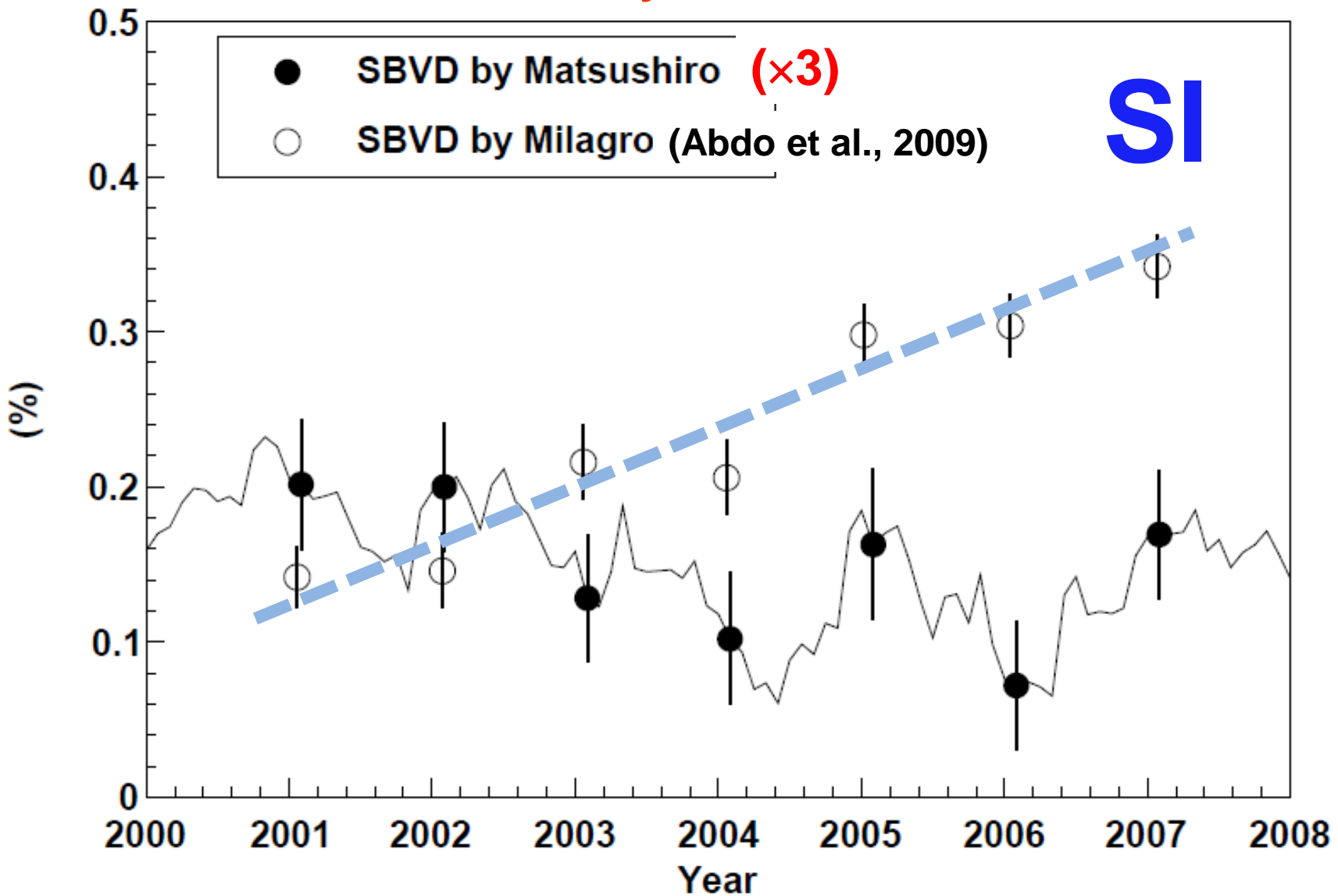


SI daily variation

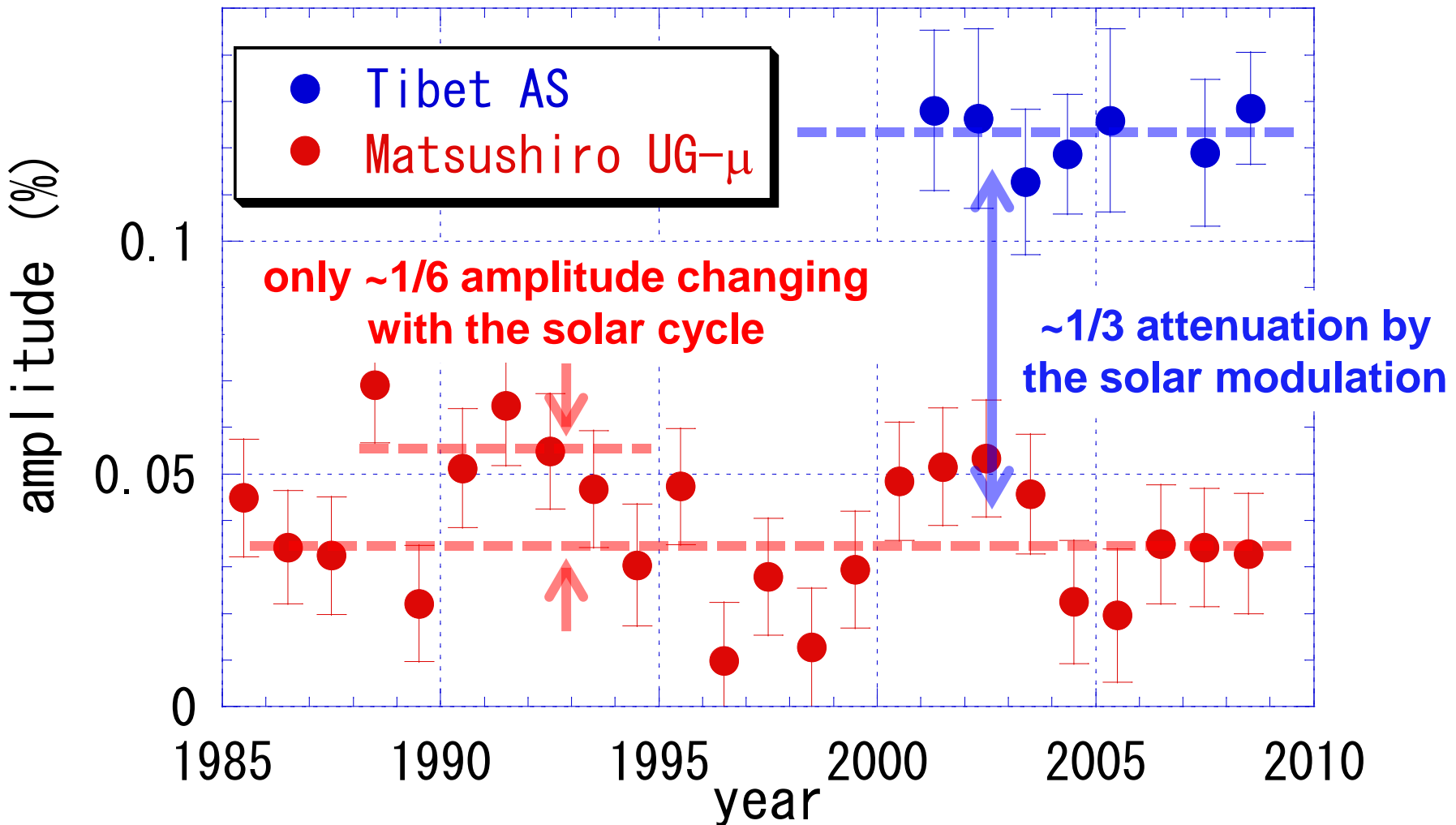


Steady increase of amplitude?

No significant correlation with the solar activity
seen by Matsushiro



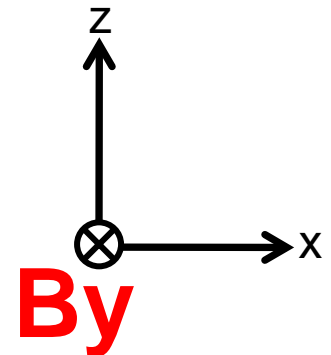
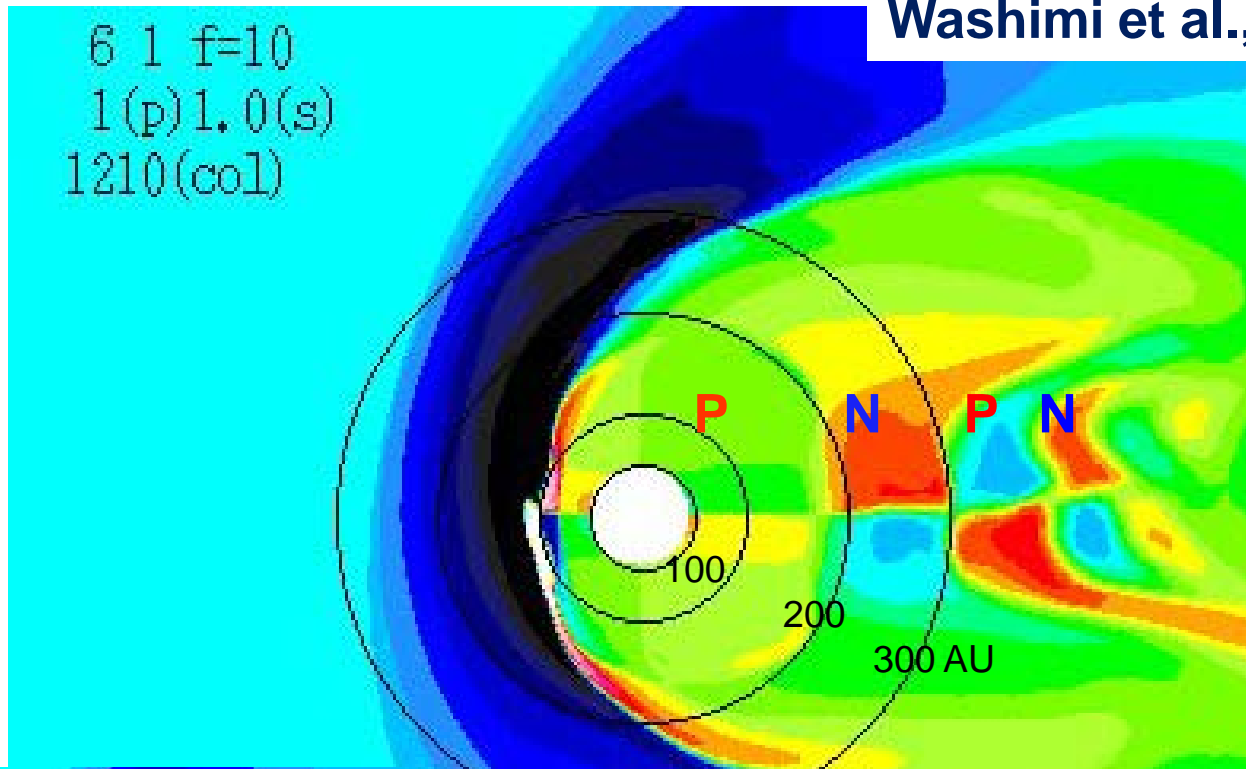
Small solar cycle variation (if any)



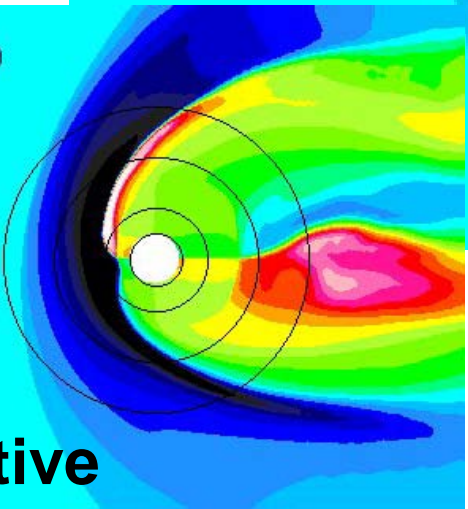
MHD model heliosphere

Washimi et al., ApJL, 670, 2007

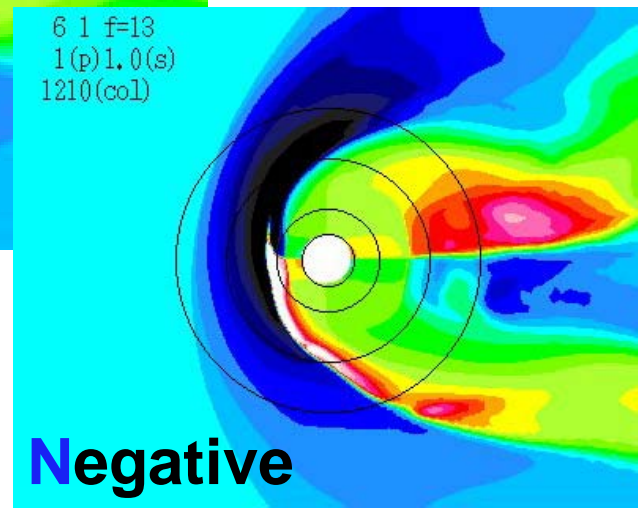
6 1 f=10
1(p)1.0(s)
1210(col)



6 1 f=15
1(p)1.0(s)
1210(col)



6 1 f=13
1(p)1.0(s)
1210(col)



Positive

Negative

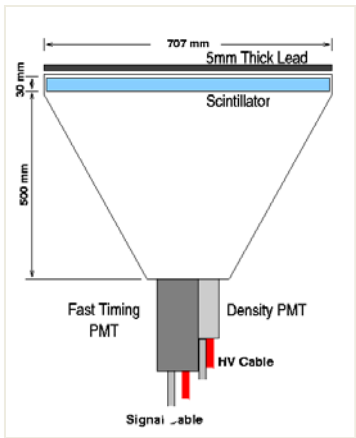
Tibet III AS Array

@Yangbajing (八羊井)
Tibet, China

90°53' E, 30°11' N

4,300 m a.s.l. (606 g/cm²)

- 37000 m² detection area
- Total 789 detectors
- Mode Energy ~ 3 TeV
- Trigger Rate ~ 1.7 kHz

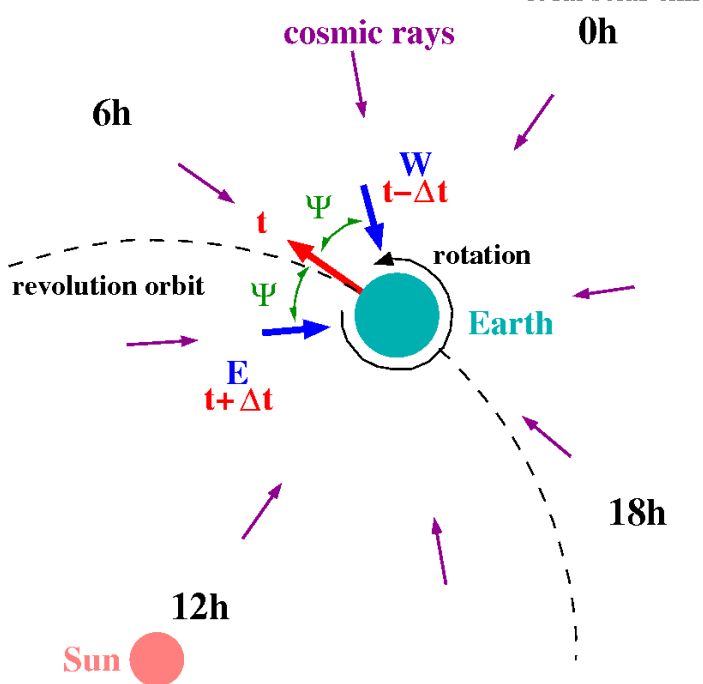
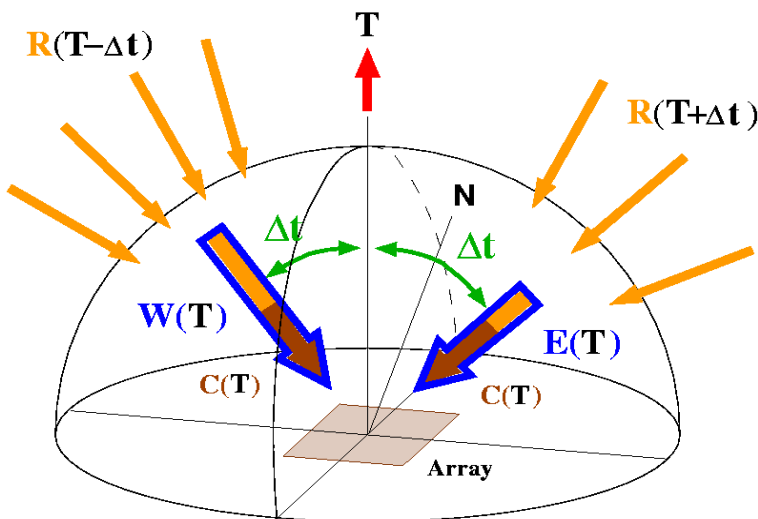


Google map



E-W Method (method I)

K.Nagashima et al., Nuovo Cimento Soc. Ital Fis. 12C, 695(1989)



$\langle I \rangle$: constant component, $I(t)$: variable component

\mathcal{R} : CR intensity outside the atmosphere, \mathcal{C} : meteorological effect

$$\begin{aligned}\langle I \rangle + I(t) &= (\langle \mathcal{R} \rangle + \mathcal{R}(t)) (\langle \mathcal{C} \rangle + \mathcal{C}(t)) \\ &= \langle \mathcal{R} \rangle \langle \mathcal{C} \rangle + \mathcal{R}(t) \langle \mathcal{C} \rangle + \langle \mathcal{R} \rangle \mathcal{C}(t) + \mathcal{R}(t) \mathcal{C}(t)\end{aligned}$$

$$\langle I \rangle \equiv \langle \mathcal{R} \rangle \langle \mathcal{C} \rangle$$

$$\begin{aligned}\frac{I(t)}{\langle I \rangle} &= \frac{\mathcal{R}(t)}{\langle \mathcal{R} \rangle} + \frac{\mathcal{C}(t)}{\langle \mathcal{C} \rangle} + \frac{\mathcal{R}(t) \mathcal{C}(t)}{\langle \mathcal{R} \rangle \langle \mathcal{C} \rangle} \\ &\approx \frac{\mathcal{R}(t)}{\langle \mathcal{R} \rangle} + \frac{\mathcal{C}(t)}{\langle \mathcal{C} \rangle} \\ &\equiv R(t) + C(t)\end{aligned}$$

$$E(t) \equiv \frac{I(t + \delta t)}{\langle I \rangle} = R(t + \delta t) + C(t)$$

$$W(t) \equiv \frac{I(t - \delta t)}{\langle I \rangle} = R(t - \delta t) + C(t)$$

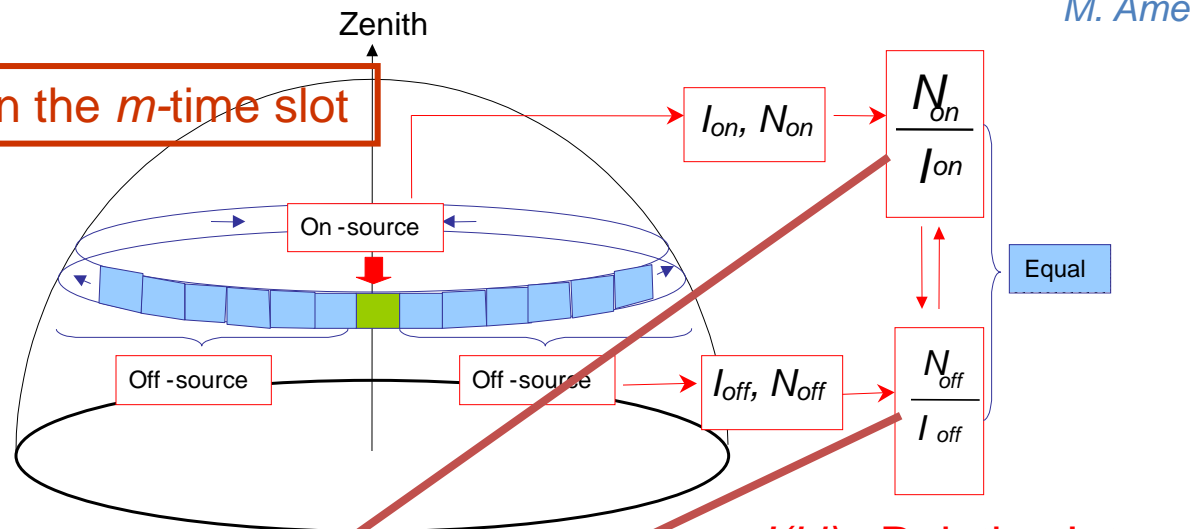
$$\begin{aligned}\underline{D(t)} &= \frac{E(t) - W(t)}{2 \delta t} \\ &= \frac{R(t + \delta t) - R(t - \delta t)}{2 \delta t} \equiv \frac{d}{dt} R(t)\end{aligned}$$

The time derivative of $R(t)$ can be obtained

- Can correct common variations including the atmospheric effect.
- Sacrifices statistical significance.

Equi-Zenith Angle Method (method II)

M. Amenomori, et al., ApJ. 633, 1005 (2005)



$$\chi^2 = \sum_{m,n,l} \left(\left\{ \frac{N_{\text{obs}}(m,n,l)}{I(i,j)} - \frac{\sum_{l' \neq l} [N_{\text{obs}}(m,n,l') / I(i',j')]}{\sum_{l' \neq l} 1} \right\}^2 \times \left\{ \frac{N_{\text{obs}}(m,n,l)}{I^2(i,j)} + \frac{\sum_{l' \neq l} [N_{\text{obs}}(m,n,l') / I^2(i',j')]}{\left(\sum_{l' \neq l} 1 \right)^2} \right\}^{-1} \right).$$

m : time ($5^\circ = 20$ minutes)

n : zenith angle (4°)

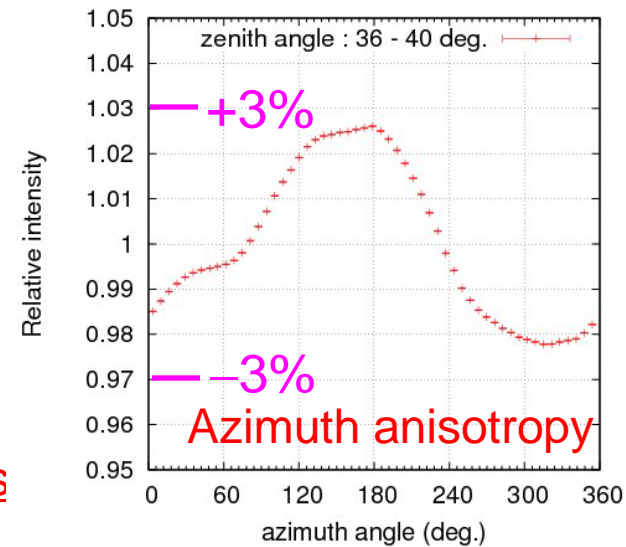
l : azimuth angle ($4^\circ / \sin(n)$)



i : right ascension (5°)

j : declination (5°)

Obtain $I(i,j)$ giving minimum χ^2



Normalize the average of $I(i, j)$ in each declination band to 1



Obtain 2D map of $I(i, j)$

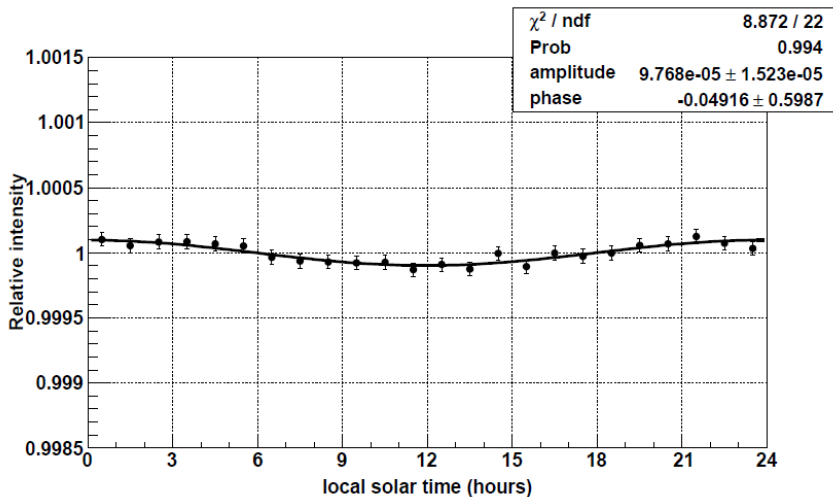
Gives $R(t)$ itself in stead of time derivative

- No sacrifice of statistical significance.
- Azimuth anisotropy must be corrected in advance.

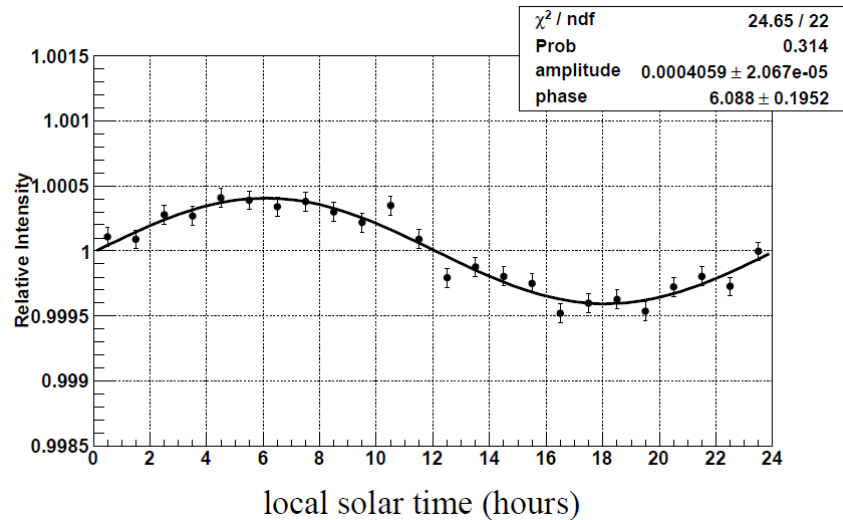
Compton-Getting effect (in solar time)

$$\alpha = (\gamma + 2) \frac{v}{c} F$$

Method I



Method II



	α ($\times 10^{-2}$ %)	ϕ [hr]	$\chi^2/\text{d.o.f.}$
(a)	4.06 ± 0.21 (3.86)	6.1 ± 0.2 (6.0)	24.65/22
(b)	0.13 ± 0.21	16.2 ± 6.2	19.53/22

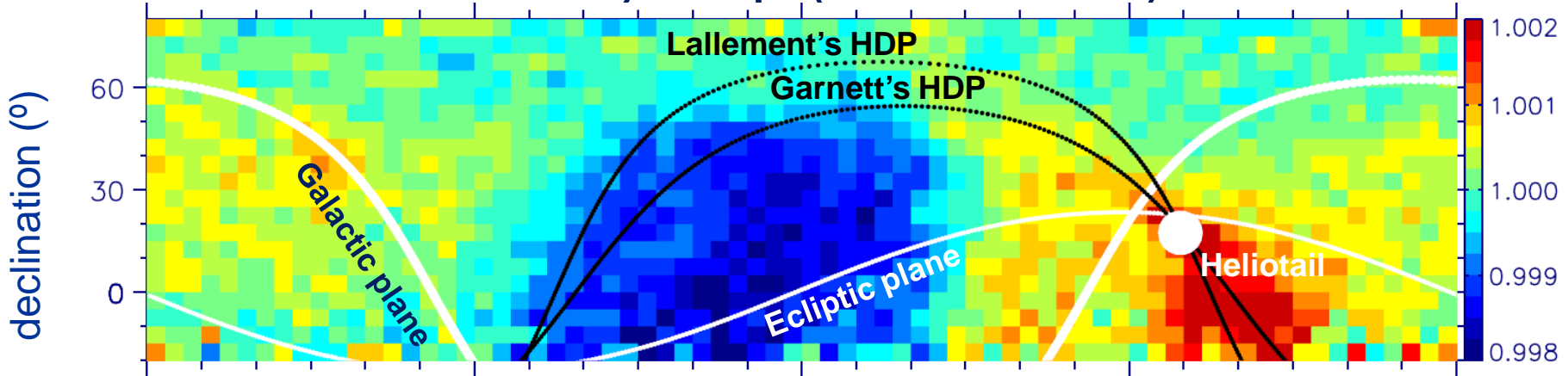
SI2 variation (367 c/y) as a measure of systematic error

Observed sidereal anisotropy

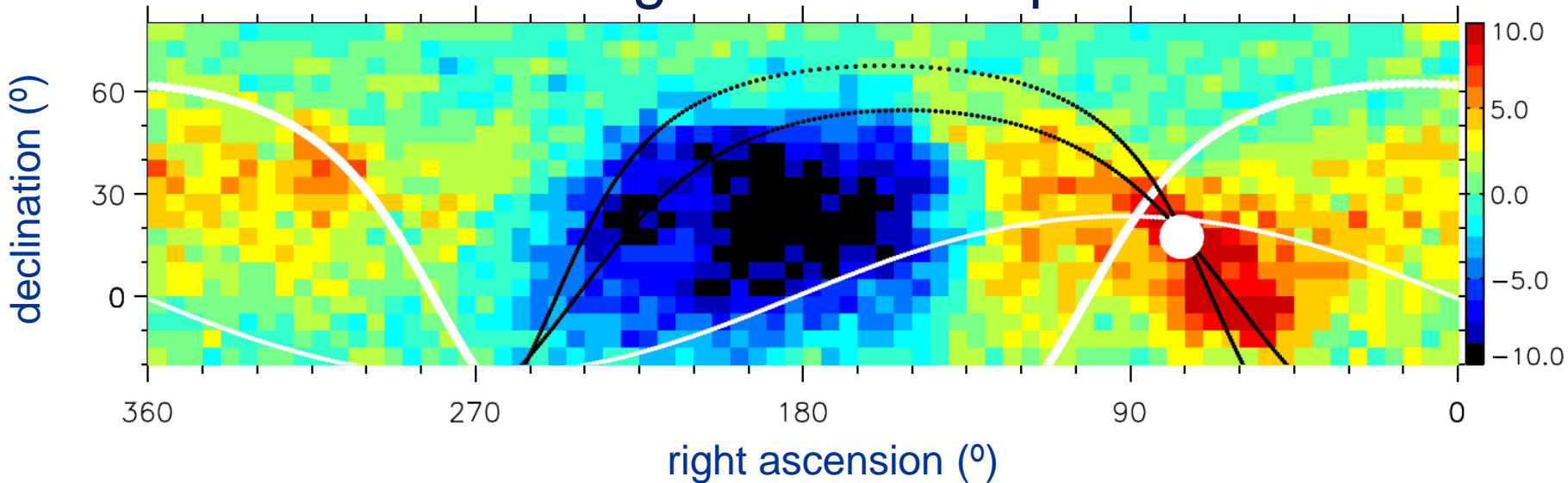
(1,916 live days in Nov. 1999 ~ Dec. 2008)

$E_{\text{mode}} = 7 \text{ TeV}$

Intensity map (normalized)

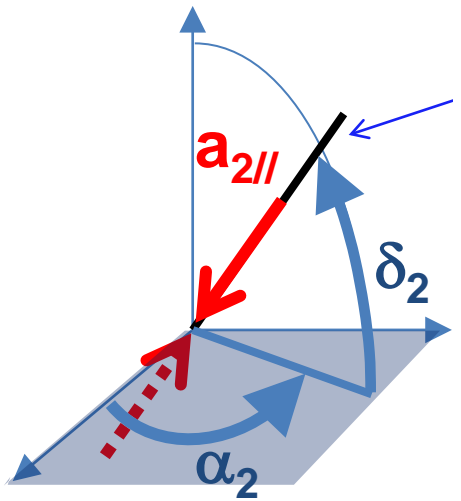


Significance map

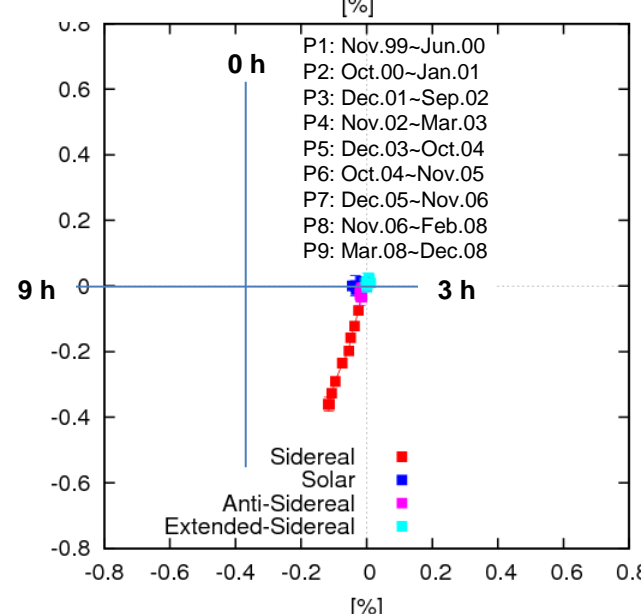
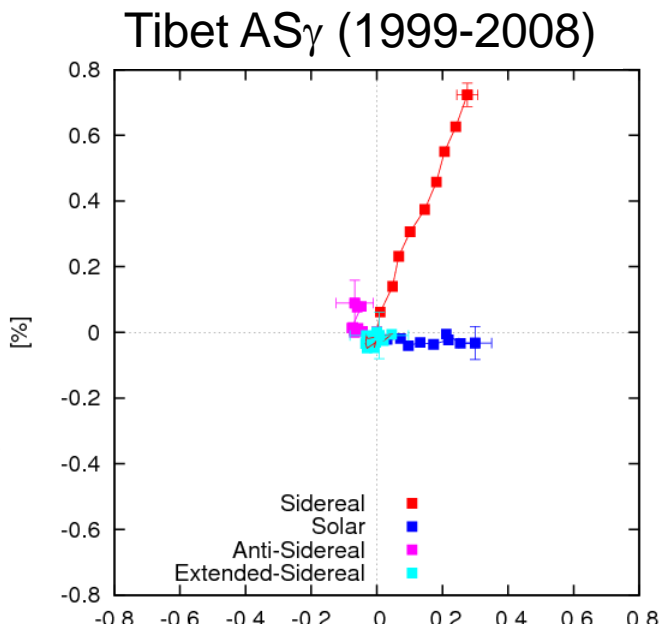
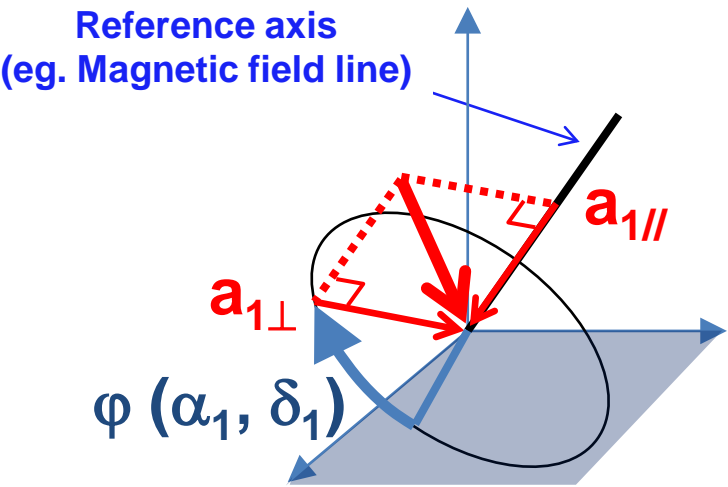


Global Anisotropy model (1/3)

Bi-Directional Flow (BDF)



Uni-Directional Flow (UDF)



Global Anisotropy model (2/3)

Origin of Uni- & Bi-directional flows

Best-fit parameters

(Amenomori et al., proc. ICRC, 2009)

Uni-directional

$$a_{1\perp} = 0.141\%, \quad a_{1\parallel} = 0.008\%$$

$$\alpha_{1\perp} = 37.5^\circ, \quad \delta_{1\perp} = 37.5^\circ$$

Bi-directional

$$a_{2\parallel} = 0.140\%$$

$$\alpha_{2\parallel} = 97.4^\circ, \quad \delta_{2\parallel} = -22.5^\circ \text{ (LIMF orientation)}$$

For 5 TeV CRs...

Larmor radius : $R_L \sim 0.002$ pc in $3\mu\text{G}$ field

Scattering m.f.p. : $\lambda_{\parallel} \sim 3$ pc

(e.g. Moskalenko et al., 2002)

$$a_{1\parallel} \sim \lambda_{\parallel} / L \sim 0.001 \quad \therefore L \sim 3 \text{ kpc}$$

Large-scale?

However...

$a_{1\parallel}$ is not significant, but $a_{1\perp}$

Bohm factor $\lambda_{\parallel} / R_L \sim 1500 \gg 1$ (~10 in the heliosphere)

\Rightarrow Perp. diffusion flux is negligible

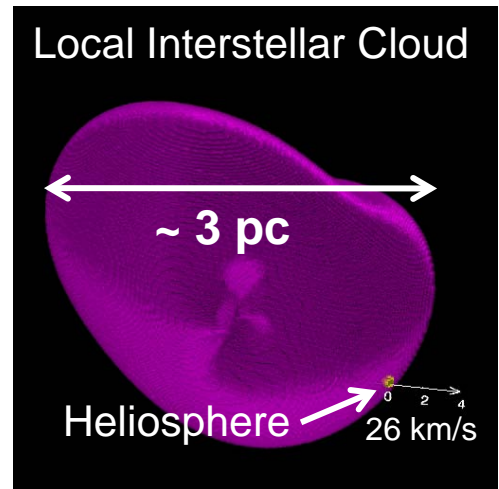
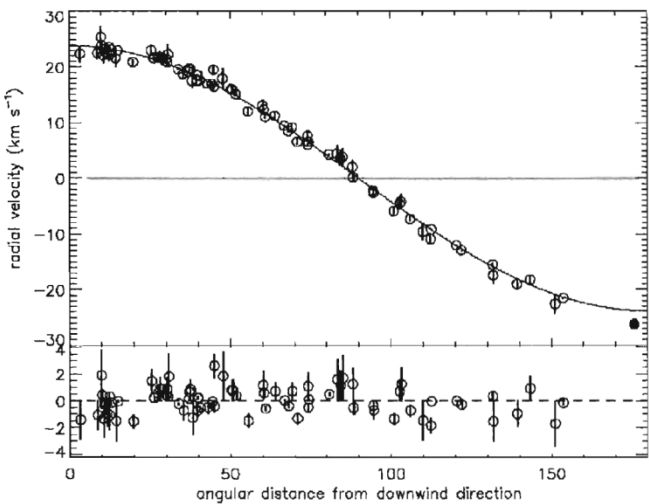
\Rightarrow Only diamagnetic drift can produce significant $a_{1\perp}$

$a_{1\perp} \sim R_L / L' \sim 0.001 \quad \therefore L' \sim 2 \text{ pc}$

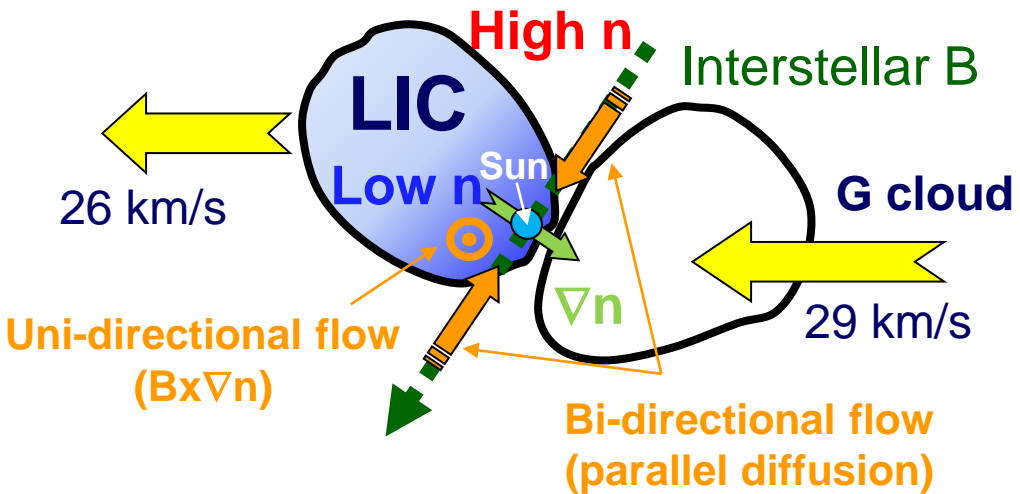
Local-scale structure is needed

Global Anisotropy model (3/3)

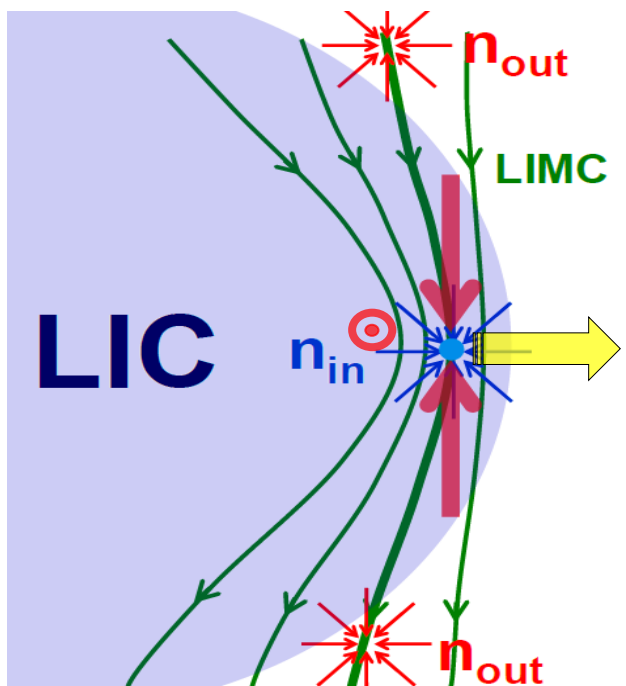
Slavin, AIP proc., 1156, 2009



Redfield & Linsky, ApJ, 534, 2000

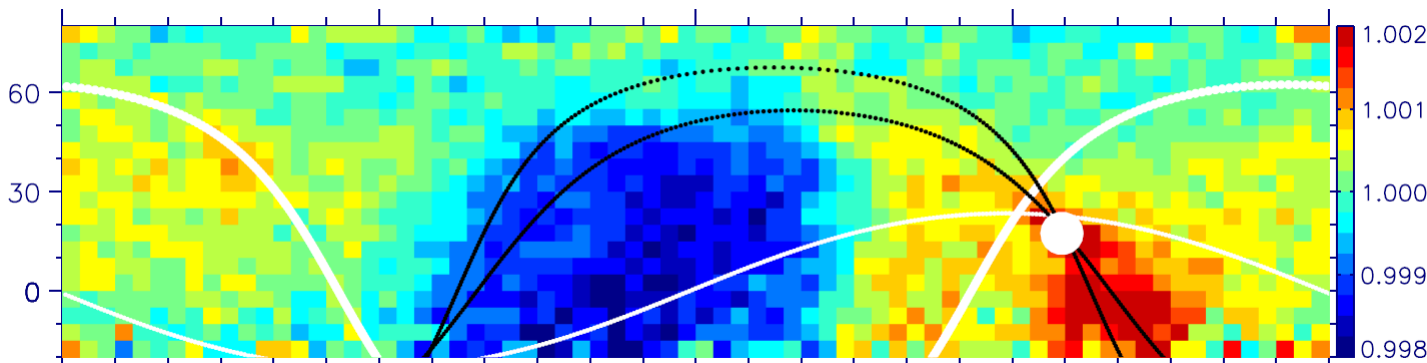


This model also allows us to infer
the polarity of B from ∇n



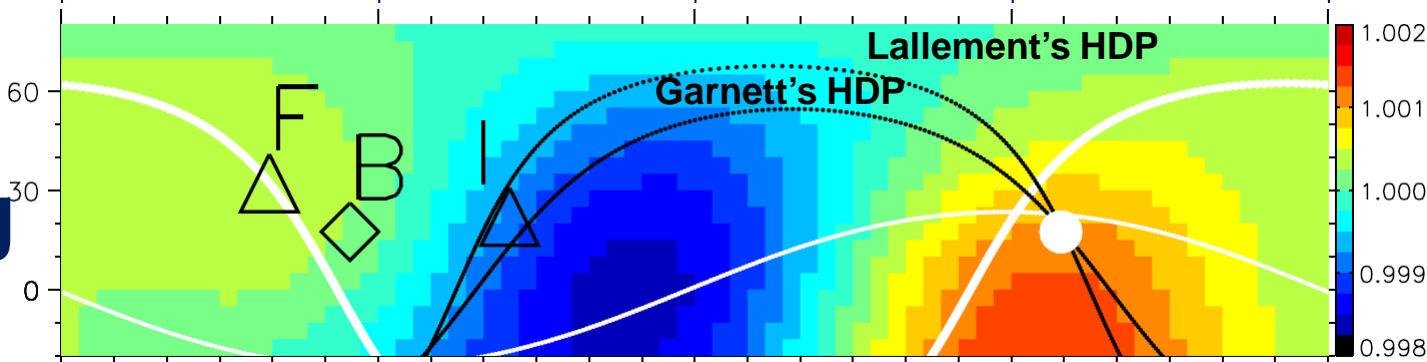
Midscale Anisotropy model (1/2)

Obs.



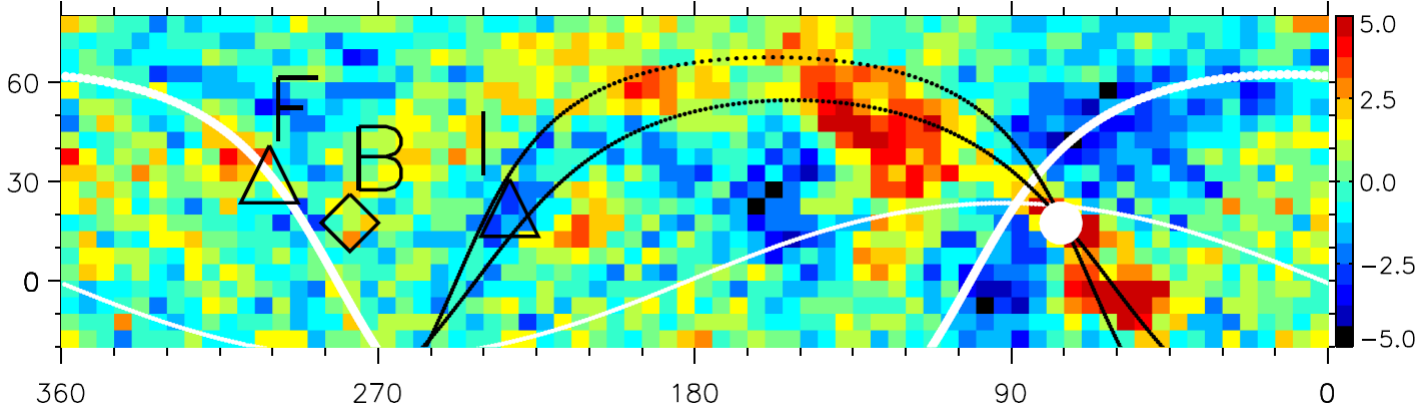
GA

Best-fitting

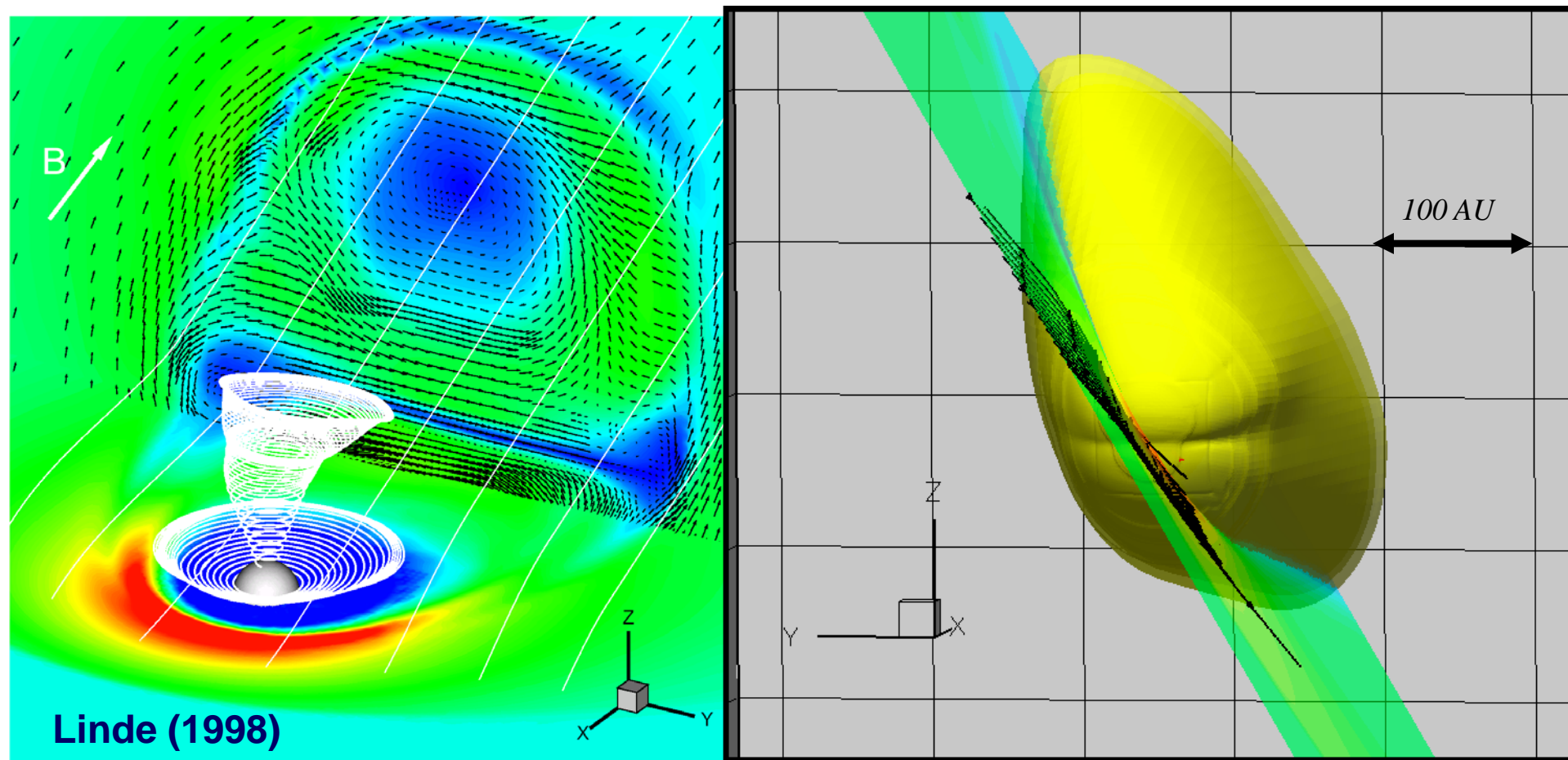


MA

Obs.- GA
(significance)

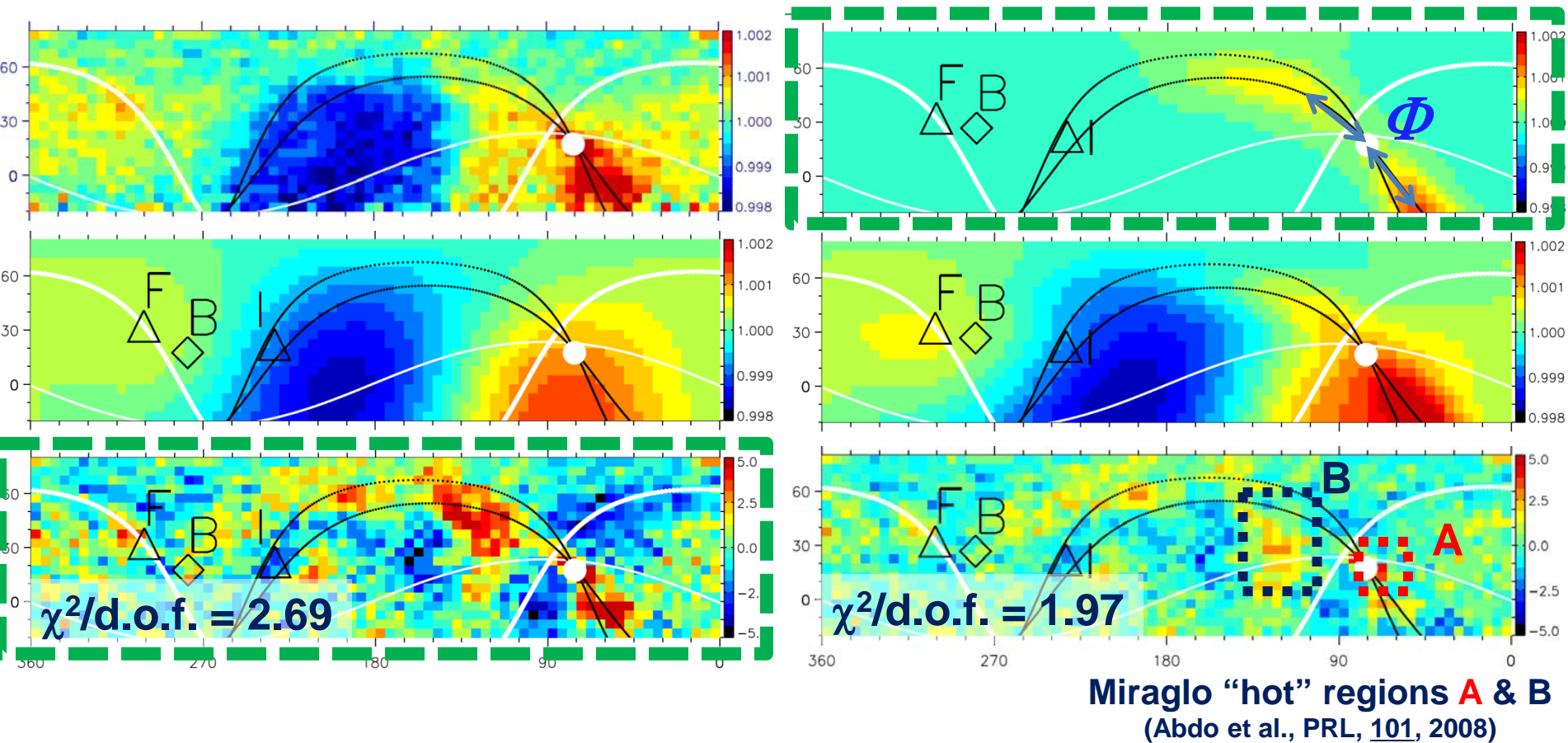


The heliosphere as seen outside the solar system: Asymmetric! (Opher, 2007)



Midscale Anisotropy model (2/2)

$$\left[b_1 \exp\left\{-\frac{(\phi_{n,m} - \Phi)^2}{2\sigma_\phi^2}\right\} + b_2 \exp\left\{-\frac{(\phi_{n,m} + \Phi)^2}{2\sigma_\phi^2}\right\} \right] \exp\left(-\frac{\theta_{n,m}^2}{2\sigma_\theta^2}\right)$$



Original intensity

UDF

Normalized intensity

+

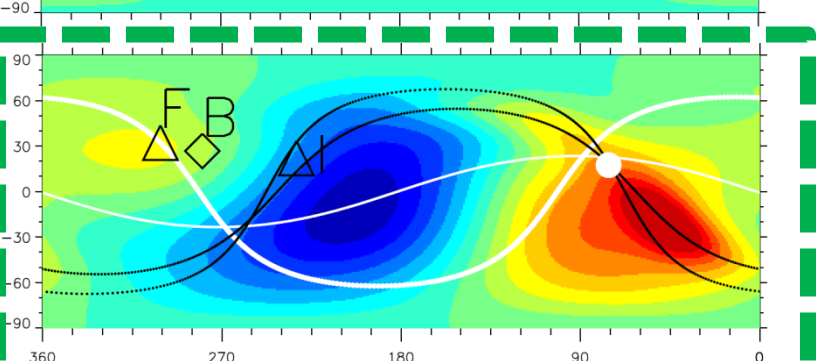
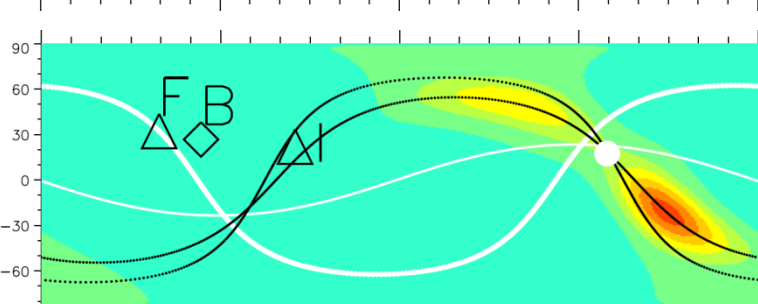
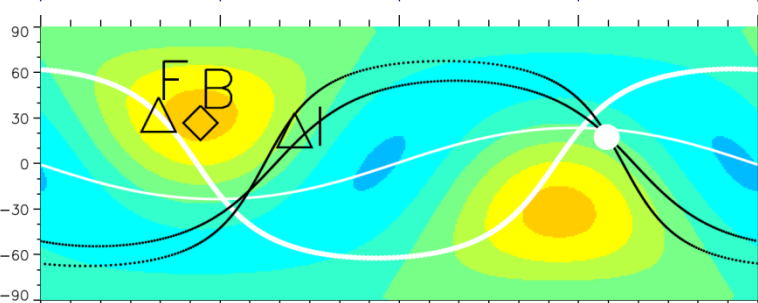
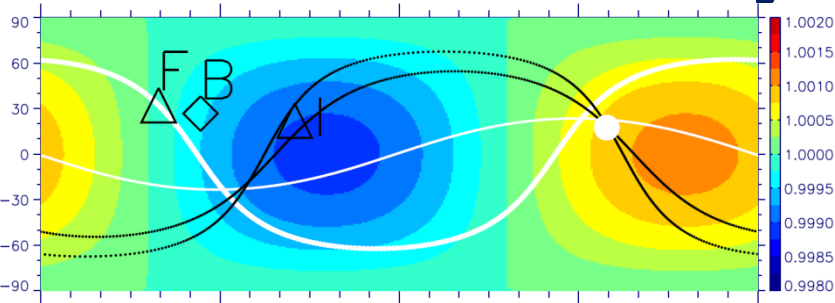
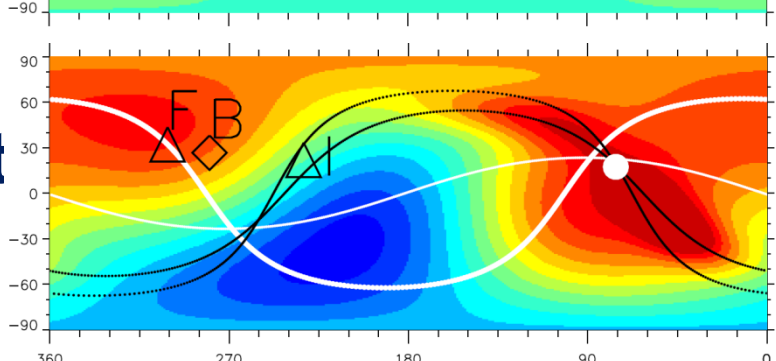
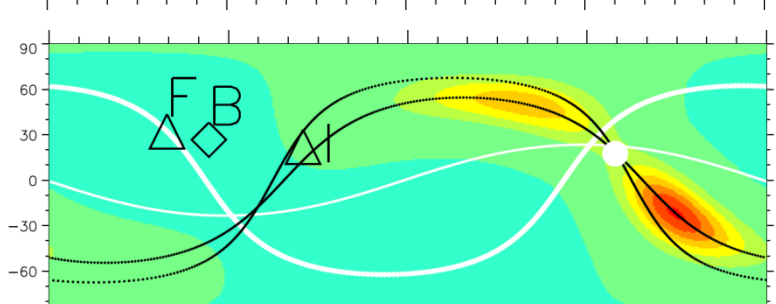
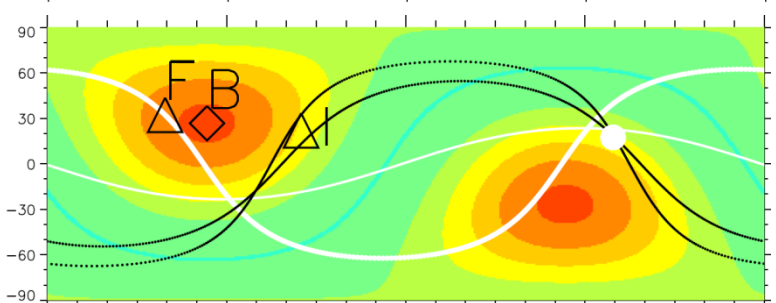
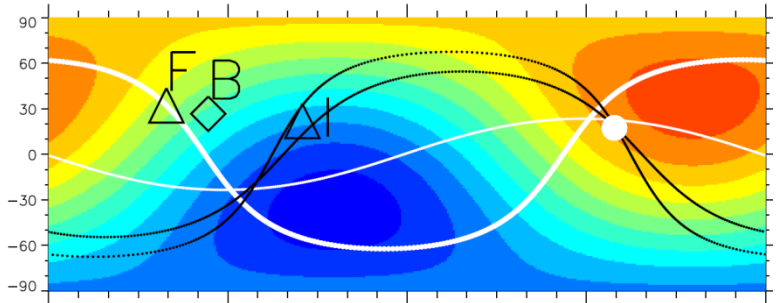
BDF

+

MA

II

Best-fit
model



Best-fit parameters

GA+MA model (with GA alone)

GA

$a_{2//}$ (%)	$\alpha_{2//}$ ($^{\circ}$)	$\delta_{2//}$ ($^{\circ}$)	$\chi^2/\text{d.o.f.} = 1.97$
0.134 ± 0.002 (0.133 ± 0.002)	99.7 ± 0.6 (98.0 ± 0.4)	-27.3 ± 1.4 (-17.5 ± 0.8)	$(\chi^2/\text{d.o.f.} = 2.69)$
$a_{1//}$ (%)	$a_{1\perp}$ (%)	$\alpha_{1\perp}$ ($^{\circ}$)	$\delta_{1\perp}$ ($^{\circ}$)
0.005 ± 0.002 (0.026 ± 0.001)	0.145 ± 0.002 (0.151 ± 0.001)	34.8 ± 0.8 (27.5 ± 0.8)	39.5 ± 0.8 (46.7 ± 0.5)

MA

b_1 (%)	b_2 (%)	$\sigma_{//}$ ($^{\circ}$)	σ_{\perp} ($^{\circ}$)	Φ ($^{\circ}$)
0.150 ± 0.013	0.095 ± 0.004	23.8 ± 0.7	11.0 ± 0.5	49.5 ± 0.9

Energy dependence (1/3)

(The energy resolution is ~50 %)

Obs.

GA

MA

E_{mode}

4.0
(TeV)

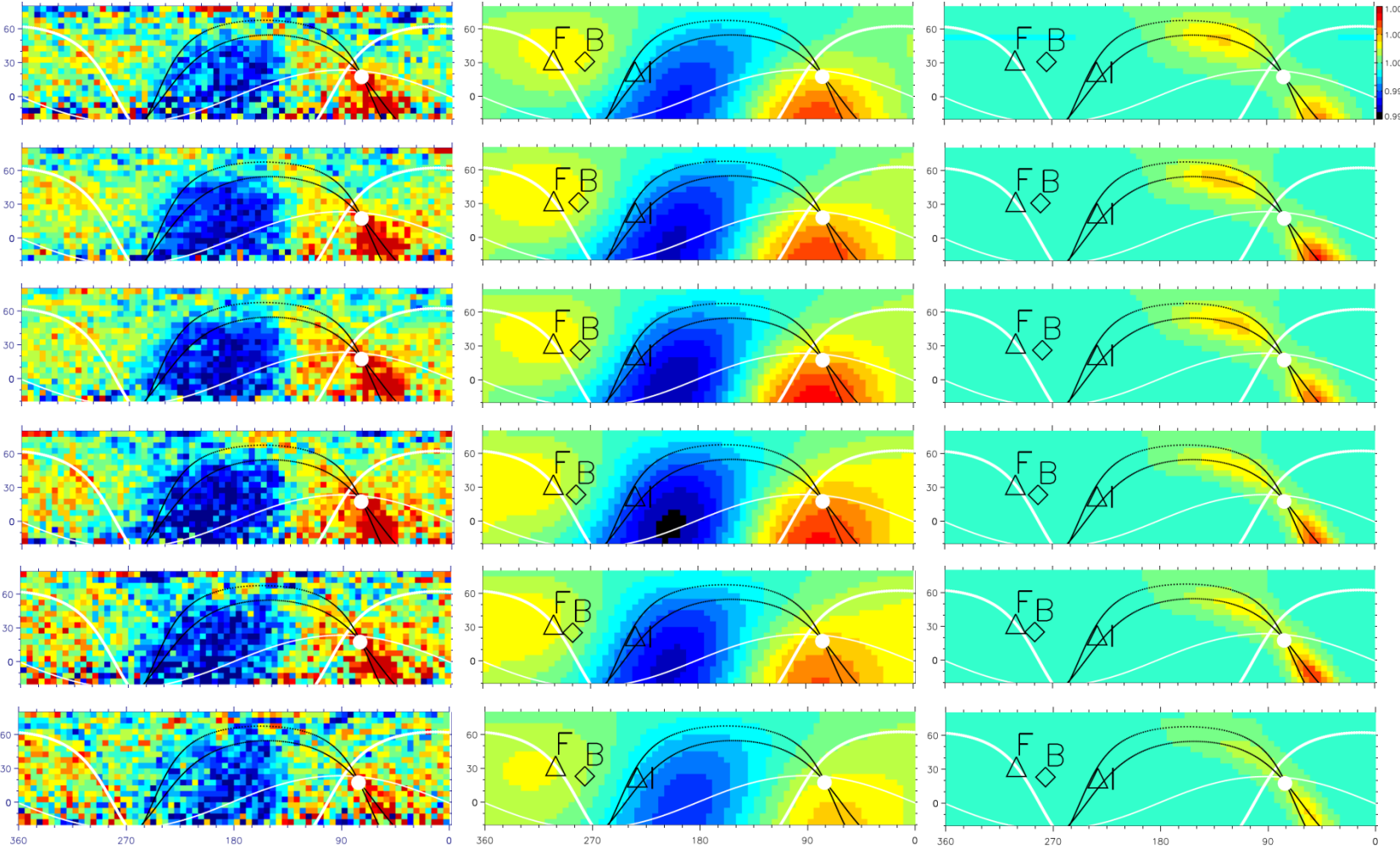
4.6

5.7

7.8

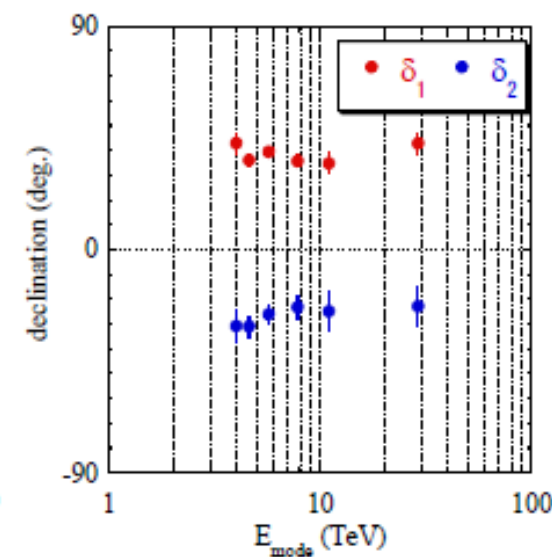
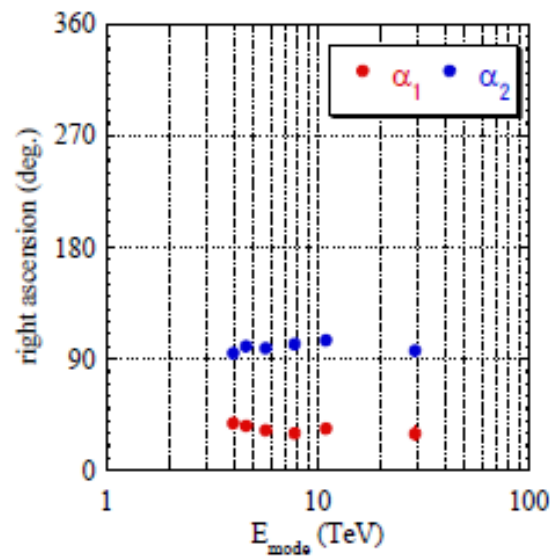
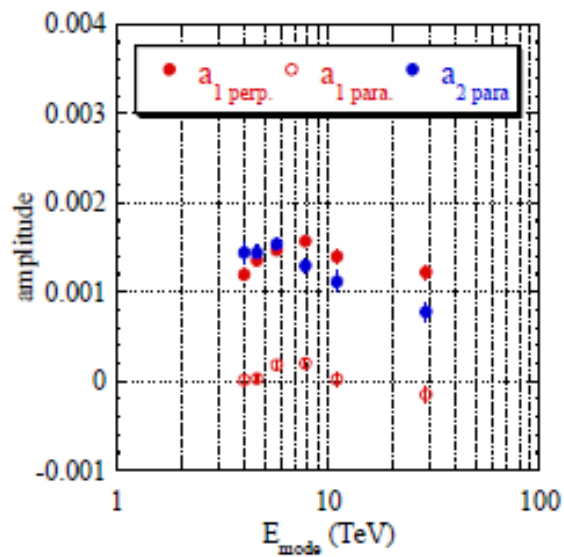
11.0

29.0

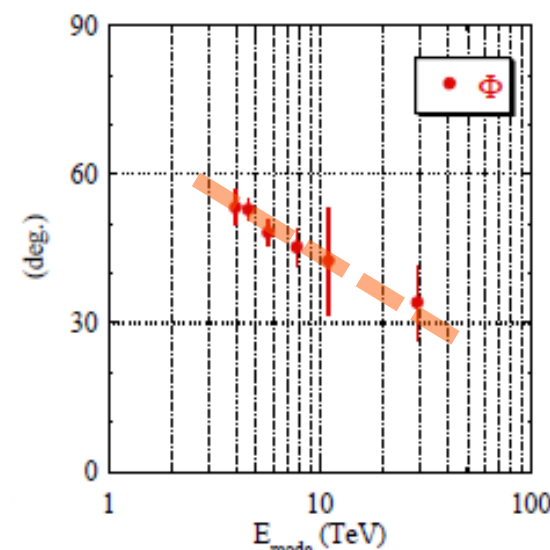
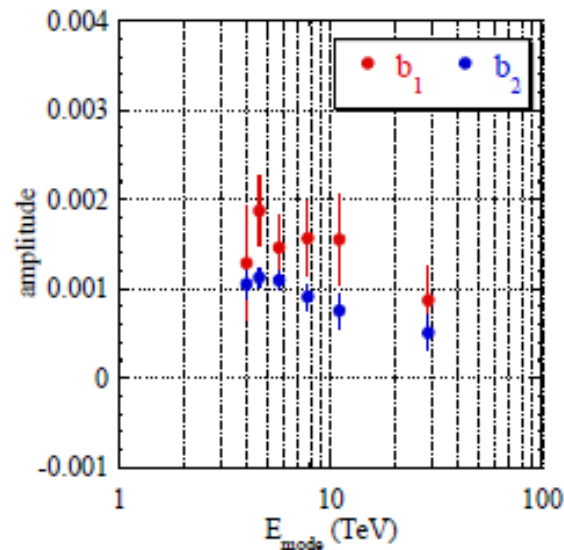


Energy dependence (2/3)

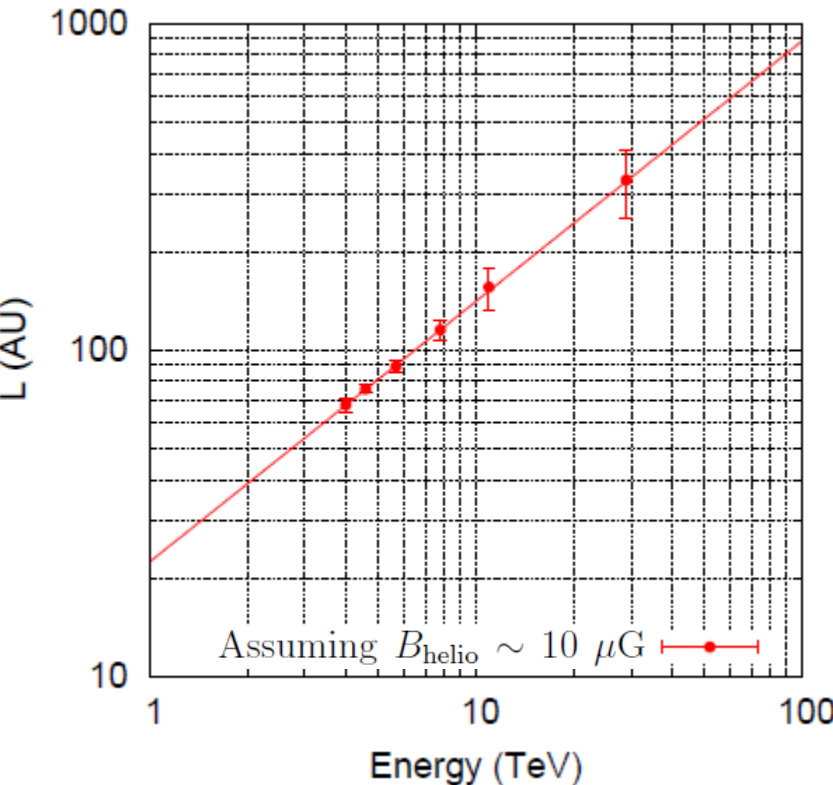
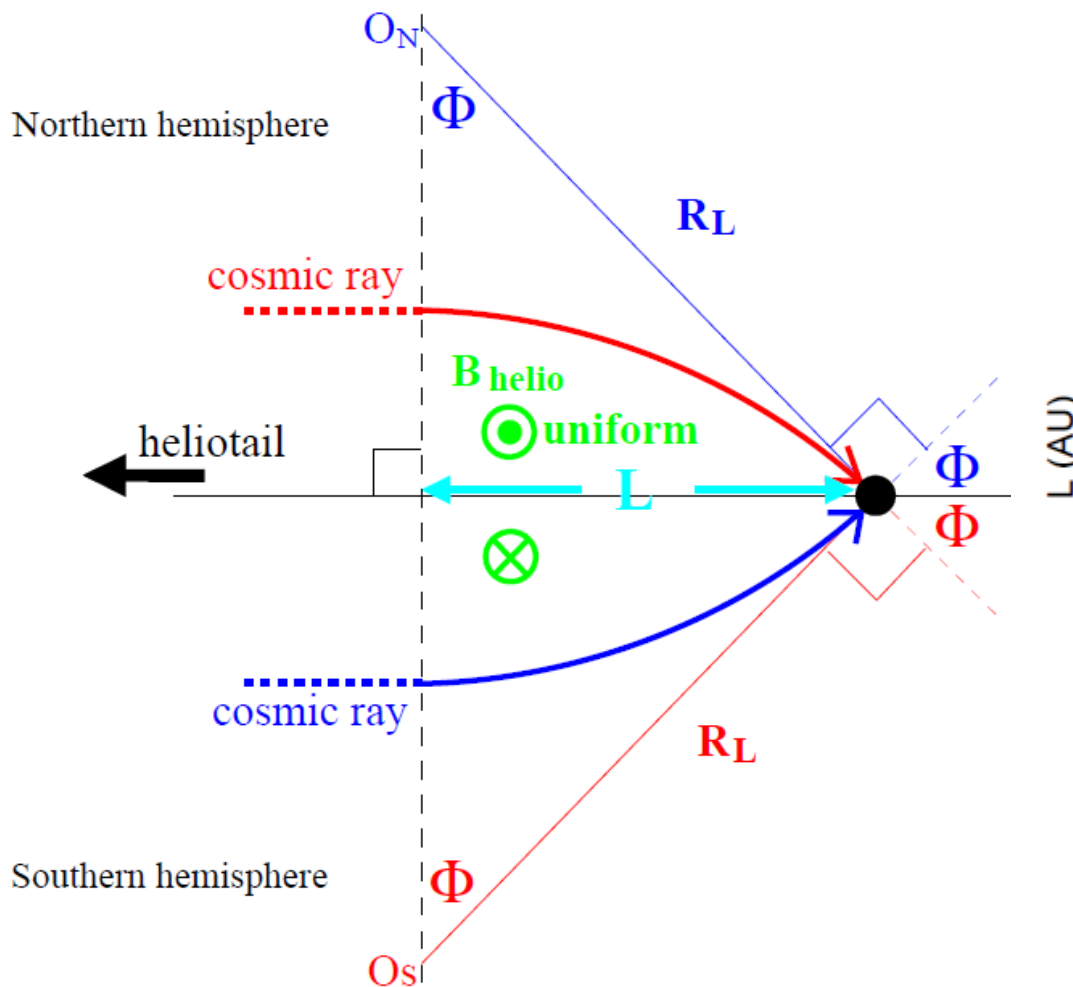
GA



MA



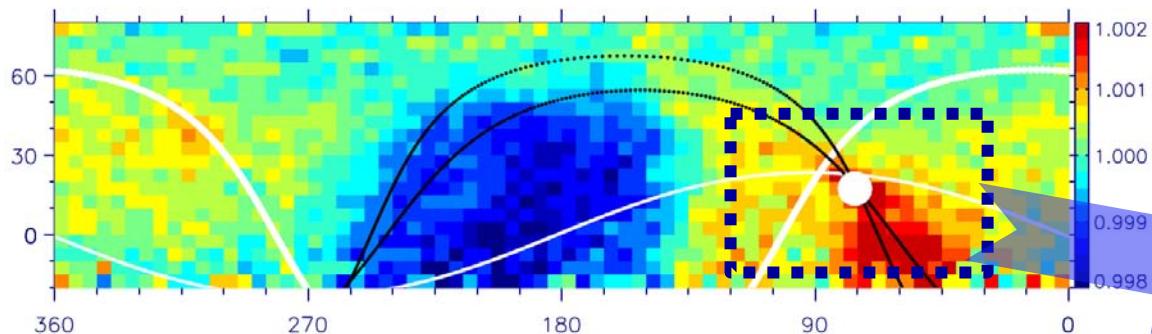
Energy dependence (3/3)



$$L \text{ [pc]} = R_L \text{ [pc]} \sin \Phi \approx \frac{E \text{ [TeV]}}{B_{\text{helio}} \text{ [\mu G]}} 10^{-3} \sin \Phi$$

Milagro hot region A

(Abdo et al., PRL, 101, 2008)



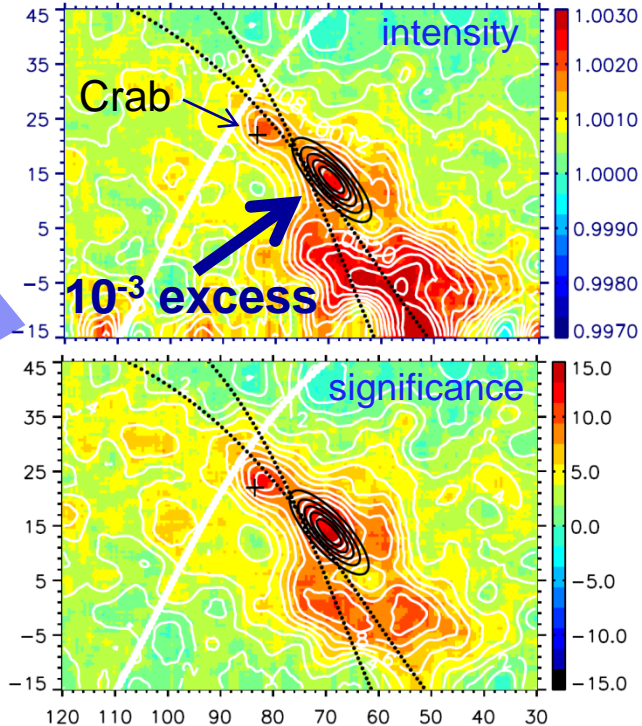
Tibet : $+14\sigma$ ($\alpha=67.5 \pm 2.5^\circ$, $\delta=17.5 \pm 2.5^\circ$)

Milagro: $+15\sigma$ ($\alpha=69.4 \pm 0.7^\circ$, $\delta=13.8 \pm 0.7^\circ$)

- 2.6° wide and 7.6° long, 46° inclined from RA axis.
 - Inconsistent with γ -ray emission (AS compactness).
 - Appears like the well-collimated hadron beam.
-
- Difficult to interpret in terms of the proton's propagation in LISMF
 - **Neutron production in the gravitationally focused tail of ISM material?**
Neutron decay length is $c\gamma\tau \sim 0.1$ pc $\gg R_L$, but the low column density of ISM can produce only an intensity excess of 10^{-10} rather than 10^{-3} .

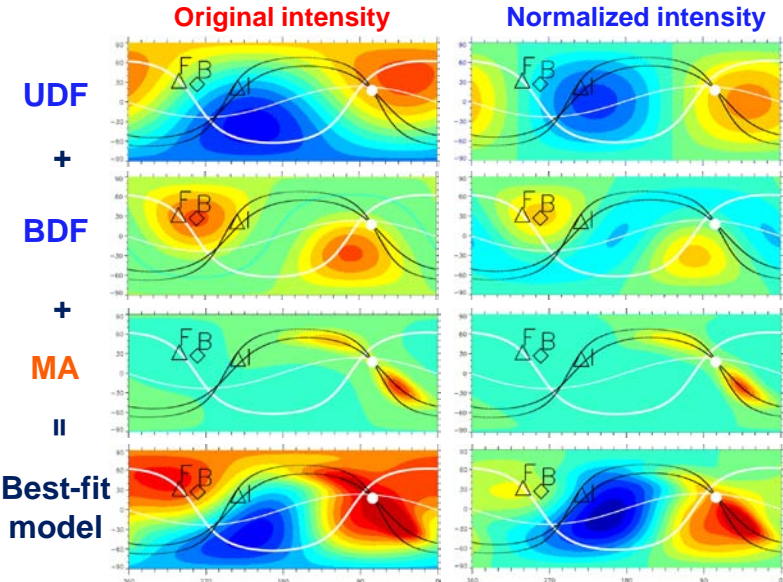
(Drury & Aharonian, arXiv:0802.4403, 2008)

This also applies to a possible idea interpreting $\sim 10^{-3}$ GA in terms of the hadronic interactions of CRs with ISM matter.

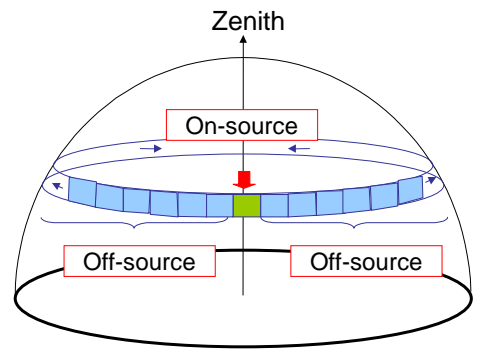


Deriving original anisotropy

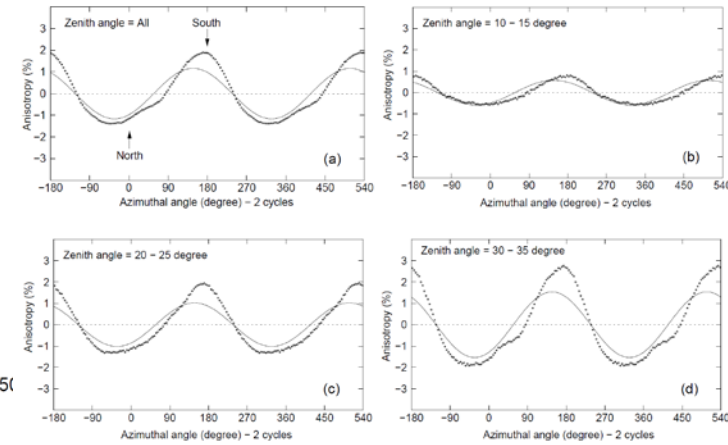
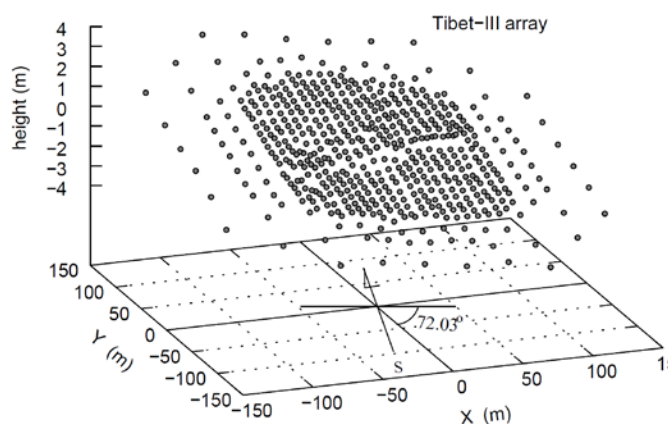
without normalization in each declination band



- In the present map, the average intensity in each declination is normalized to unity.
- For deriving original anisotropy, the azimuth distribution must be corrected for all systematic effects at $\sim 10^{-3}$ accuracy.
- Tibet AS-array normal is inclined for 1.3° toward south-west direction, causing a 10^{-2} systematic effect.
- Correction seems to be still possible.

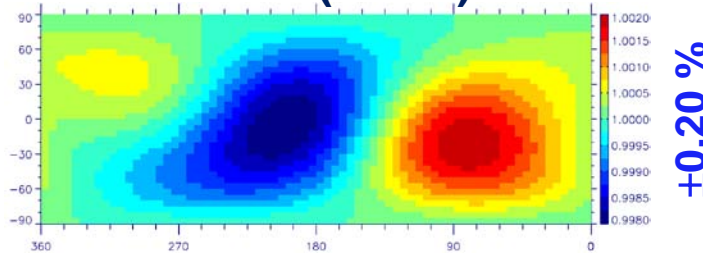


Equi-Zenith Angle Method

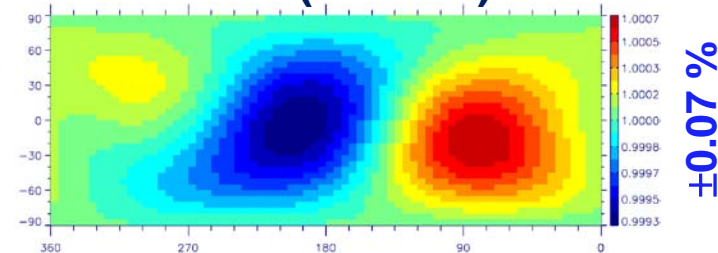


Two-hemisphere observations

Tibet (7 TeV)



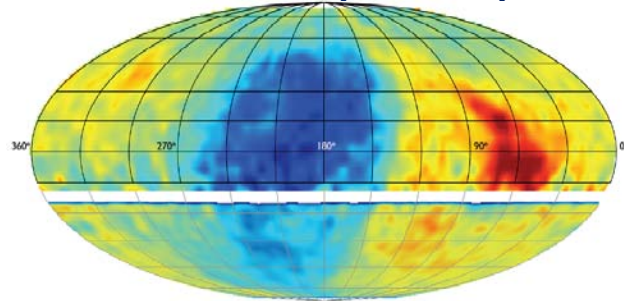
THN (0.5 TeV)



- Best-fit models of GA are very similar to each other, except 1/3 amp. by THN.

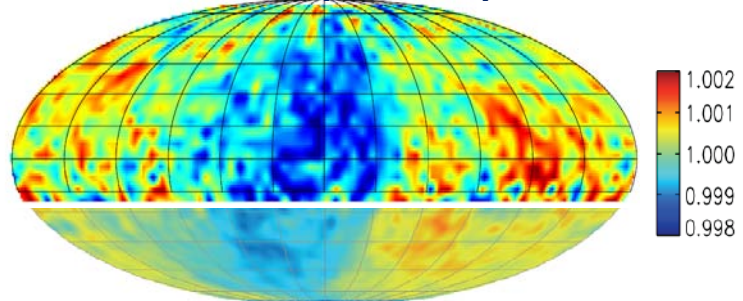
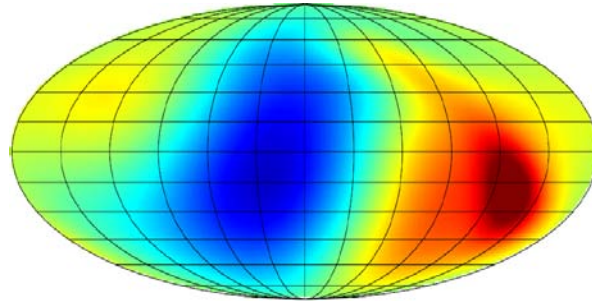
Tibet (7 TeV)
Ice Cube (20 TeV)

Data



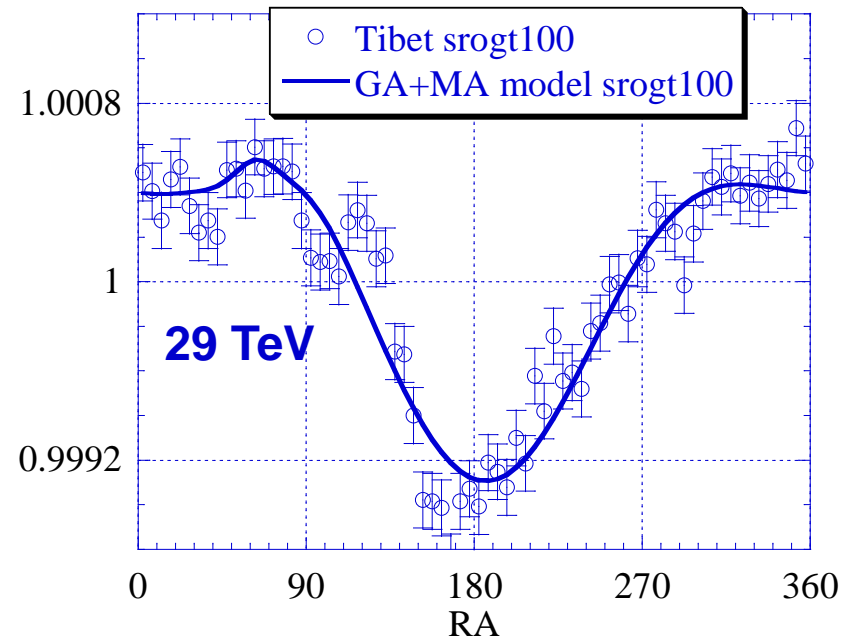
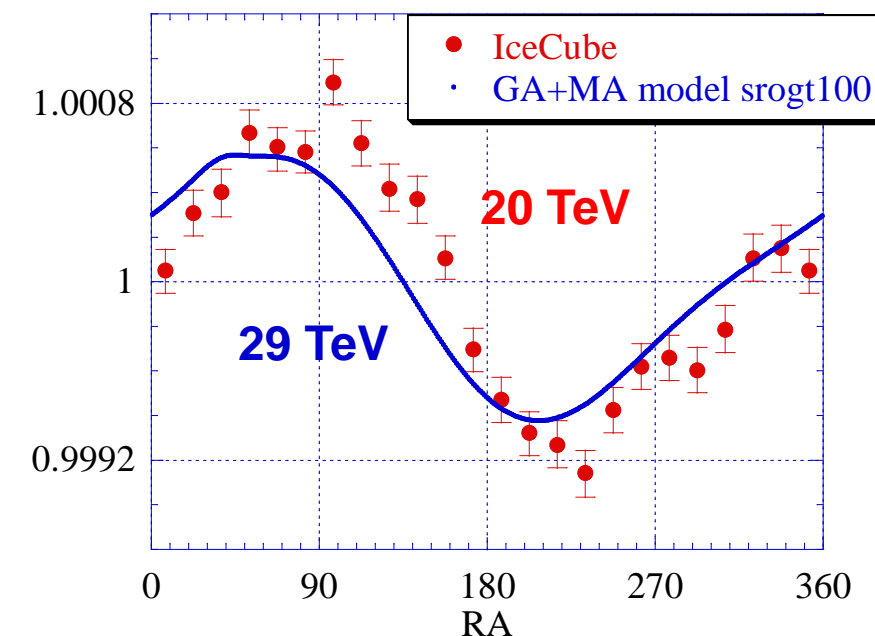
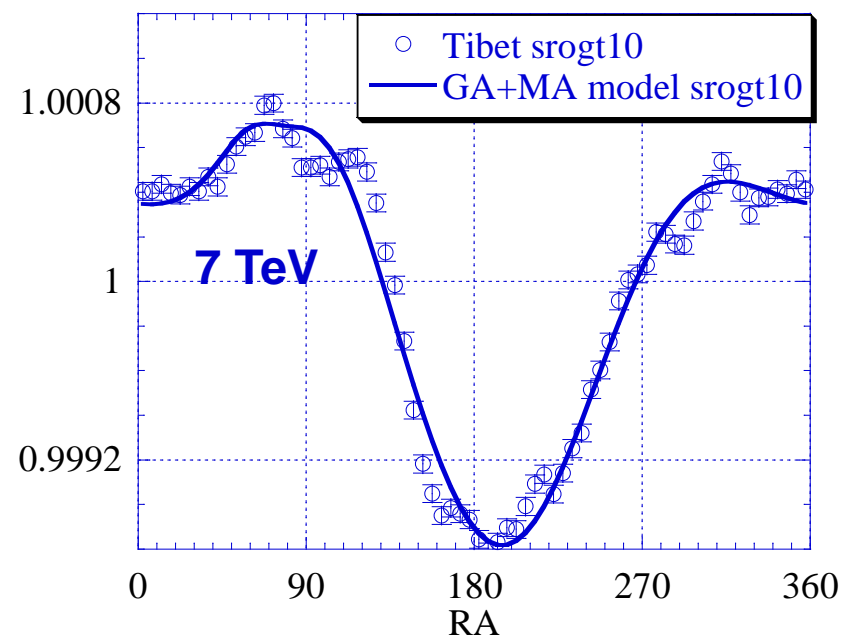
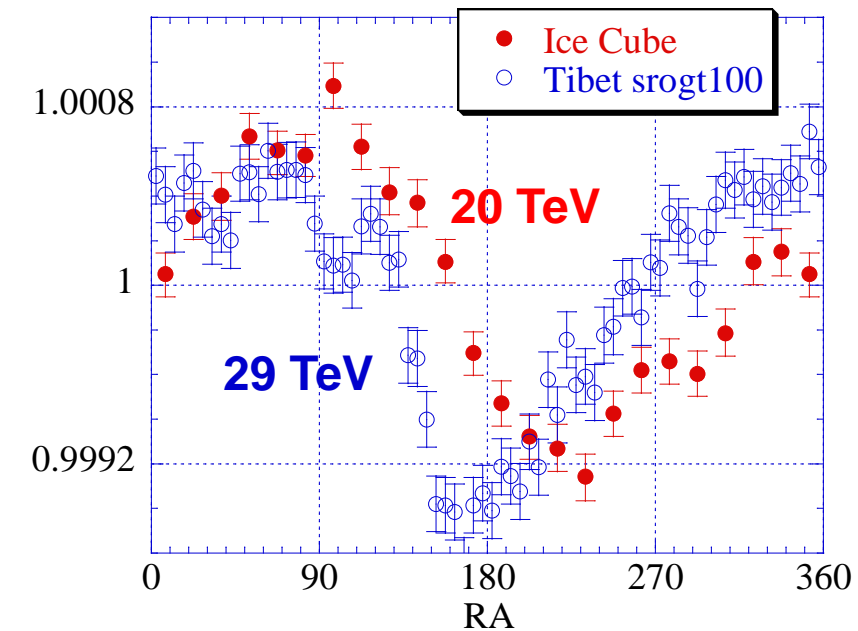
Tibet (29 TeV)
Ice Cube (20 TeV)

GA+MA model
for Tibet



1.002
1.001
1.000
0.999
0.998

- Need more statistics for quantitative comparison between Tibet & Ice Cube.



Summary

- Sidereal anisotropy by Tibet AS and UG-muon observations (SK & THN) are consistent with each other, implying minor contribution from γ -rays to the global anisotropy.
- Sidereal anisotropy by Tibet AS and THN are consistent with each other, implying the modeling with Tibet data in a single hemisphere is not seriously biased.
- THN observed a time-dependent attenuation (~1/3) of amplitude due to the solar modulation, while the anisotropy by Tibet is fairly constant.
- Sidereal anisotropy by Tibet AS is well modeled in terms of GA and MA, representing modulations in the LISMF and in the heliotail, respectively.
- The contribution from γ -rays to the anisotropy by Tibet should be identified and discriminated, quantitatively, e.g. Milagro's hot region A \Rightarrow Tibet MD project.
- For better understanding the origin of the anisotropy, the present analysis method must be improved to derive the “original” anisotropy without the normalization in each declination band.
- Two hemisphere observations by Tibet and Ice Cube should be encouraged.